

ANALYTIC AXISYMMETRIC GALAXY MODELS WITH THREE INTEGRALS OF MOTION

HERWIG DEJONGHE AND TIM DE ZEEUW

Institute for Advanced Study

Received 1987 December 11; accepted 1988 March 30

ABSTRACT

We investigate a family of inhomogeneous axisymmetric mass models with a simple gravitational potential originally introduced by Kuzmin, and subsequently studied by Kuzmin and Kutuzov. Properties of the mass models are presented, for both the oblate and the prolate sequences. Their spherical limit is Hénon's isochrone.

The density distribution $\rho(\varpi, z)$ of the models is stratified approximately on spheroids and can be written explicitly as $\rho(\varpi, \psi)$, where ψ is the gravitational potential and (ϖ, z) are cylindrical coordinates. This fact makes it possible to use a standard inversion technique in order to obtain—in closed form—the unique distribution function $F(E, L_z^2)$ that depends only on the two classical integrals of motion (the energy E and the component L_z of the angular momentum parallel to the symmetry axis) and that is consistent with the density. This F is nonnegative for all oblate models in the sequence, and also for the prolate models with central axis ratio smaller than 1.35. The resulting intrinsic velocity dispersions are given explicitly.

The potential of all these models is of Stäckel form, so that all orbits in them have an exact third integral of motion I_3 , which can be regarded as a generalization of the total angular momentum integral of the spherical limit. We present a new method for the analytical construction of distribution functions $F(E, L_z^2, I_3)$, and apply it to these mass models. We write F as the sum of two parts: $F(E, L_z^2, I_3) = F_1(E, L_z^2) + F_2(E, L_z^2, I_3)$, where F_2 is a power series in E, L_z^2 , and I_3 . We choose a simple form for F_2 , compute the resulting density and subtract it from the given ρ . The remaining density is then reproduced by F_1 , which is obtained by the standard inversion technique. This produces—for the first time—exact analytic distribution functions for realistic axisymmetric models that depend on all three integrals of motion. Kinematic properties of the models are presented, and observables are calculated.

Subject headings: galaxies: internal motions — galaxies: structure — stars: stellar dynamics

I. INTRODUCTION

Realistic dynamical models for galaxies should have velocity distributions that are anisotropic and, hence, have phase-space distribution functions that generally depend on three isolating integrals of motion. This was established for our own Galaxy in the early part of this century, through the work of Kapteyn, Schwarzschild, and Jeans, and led to the search for the famous third integral of Galactic dynamics (see Oort 1965). In the last decade it has become evident that our Galaxy is not exceptional in this respect, and that elliptical galaxies require similar models (Binney 1978; Davies 1987).

For axisymmetric models two classical integrals exist, the orbital energy E and the component L_z of the angular momentum parallel to the symmetry axis. No general expression exists for the third integral I_3 . It is therefore not surprising that the number of three-integral models is rather limited. The few available models have been constructed numerically (Richstone 1980, 1984; Levison and Richstone 1985a, b), or employ an approximate third integral (e.g., Petrou 1983a, b). For triaxial systems only the energy E is a classical integral. Models that include nonclassical integrals I_2 and I_3 have been constructed by approximate numerical techniques (Schwarzschild 1979, 1982; Vietri 1986; Levison and Richstone 1987). A review of all existing nonspherical dynamical models has been given by de Zeeuw (1987).

Many axisymmetric and triaxial mass models exist with a gravitational potential of Stäckel form, for which the Hamilton-Jacobi equation separates in ellipsoidal coordinates (Kuzmin 1956, 1973; de Zeeuw 1985a, hereafter Z85). Every orbit in such a model possesses three exact isolating integrals of motion, E, I_2 , and I_3 , which are known explicitly. I_2 and I_3 are related to the angular momentum integrals that exist in the spherical and axisymmetric limits. The orbital structure in these models resembles closely that in elliptical galaxies, and also that in our own Galaxy (Dejonghe and de Zeeuw 1988). Numerical distribution functions for a complete family of Stäckel models have been constructed recently (Bishop 1986; Statler 1987).

Many properties of the Stäckel models can be given in analytic form. It is therefore natural to ask whether analytic distribution functions can be derived for these models. This is not to be expected in general, since every spherical potential is of Stäckel form, and even for these only a limited number of families of analytic dynamical models have been constructed (e.g., Dejonghe 1984). Nevertheless, it is worthwhile to search for analytic models, since they provide insight in the internal dynamical structure of galaxies that is not so easy to obtain with numerical or approximate models. A first step in that direction was taken recently by Bishop (1987) and de Zeeuw (1988), who showed that in the special case where all stars are on infinitesimally thin tube orbits, the distribution function can be constructed analytically for an arbitrary oblate Stäckel model, by a simple inversion of a one-dimensional Abel type integral equation. The kinematic properties of these models can be found by simple quadratures.

In this paper we investigate whether more general analytic models can be constructed. We concentrate on axisymmetric models, for two reasons. The problem is somewhat simpler than the corresponding one for triaxial models, and we can use the elaborate

mathematical apparatus that is now available for the construction of two-integral axisymmetric models (Dejonghe 1986, hereafter D86). In particular, we investigate a generalization of one such technique, Fricke's (1952) method, and show that, when suitably modified, this can indeed produce completely analytic dynamical models with a distribution function that depends on all three integrals of motion. We apply this method to an axisymmetric generalization of Hénon's (1959) isochrone, which was introduced by Kuzmin (1956), and further studied by Kuzmin and Kutuzov (1962).

The construction of exact three-integral models requires a considerable amount of mathematics. The reader who is primarily interested in the observable properties of the resulting models should turn to § V.

II. DEFINITIONS AND NOTATION

In this section we collect some basic properties of axisymmetric Stäckel models. Further details can be found in Z85.

a) Spheroidal Coordinates

In order to avoid a separate treatment for oblate and prolate models, our choice of the fundamental spheroidal coordinate system differs from that used in Z85. We define spheroidal coordinates as the triple (λ, ϕ, ν) , where ϕ is the azimuthal angle in ordinary cylindrical coordinates $(\varpi = (x^2 + y^2)^{1/2}, \phi, z)$, and λ and ν are the roots for τ of

$$\frac{\varpi^2}{\tau + \alpha} + \frac{z^2}{\tau + \gamma} = 1. \quad (2.1)$$

A choice of the focal distance $\Delta = (|\gamma - \alpha|)^{1/2}$ fixes the spheroidal coordinate system. The values of α and γ are then determined apart from an additive constant. We take both of them smaller than zero. Moreover, we shall assume $0 \leq \nu \leq \lambda$. The coordinate surfaces are spheroids ($\lambda = \lambda_0$) and hyperboloids of revolution ($\nu = \nu_0$) with the z -axis as rotation axis. The relations between (λ, ν) and (ϖ, z) are given by

$$\varpi^2 = \frac{(\lambda + \alpha)(\nu + \alpha)}{\alpha - \gamma}, \quad z^2 = \frac{(\lambda + \gamma)(\nu + \gamma)}{\gamma - \alpha}. \quad (2.2)$$

Instead of α and γ we often use a and c defined by

$$\alpha = -a^2, \quad \gamma = -c^2. \quad (2.3)$$

When $a > c$, so that $c^2 \leq \nu \leq a^2 \leq \lambda$, the spheroids of constant λ are prolate, while the hyperboloids of constant ν have two sheets. λ and ν are elliptic coordinates in each meridional plane $\phi = \phi_0$, with foci on the z -axis at $z = \pm \Delta$.

When $a = c$, the spheroids become spheres, and the hyperboloids all degenerate to their asymptotic cones. Equation (2.1) now has only one root $\lambda = r^2 + a^2$, with $r^2 = x^2 + y^2 + z^2$.

When $a < c$, so that $a^2 \leq \nu \leq c^2 \leq \lambda$, the spheroids are oblate. The hyperboloids crossed their asymptotic cones and are now hyperboloids of one sheet. λ and ν again are elliptic coordinates in each meridional plane $\phi = \phi_0$, but now with foci on the ϖ -axis at $\varpi = \Delta$; i.e., there is a focal circle in the equatorial plane.

Spheroidal coordinates are degenerate cases of ellipsoidal coordinates (λ, μ, ν) , defined as the three roots for τ of

$$\frac{x^2}{\tau + \alpha} + \frac{y^2}{\tau + \beta} + \frac{z^2}{\tau + \gamma} = 1, \quad (2.4)$$

where α, β , and γ are constants, and $-\gamma \leq \nu \leq -\beta \leq \mu \leq -\alpha \leq \lambda$ (see Z85). In this convention, the coordinates degenerate differently to oblate spheroidal coordinates and to prolate spheroidal coordinates. In the former case, the x -axis is the symmetry axis, while in the latter case the z -axis is the symmetry axis. Although this is natural for a description of triaxial systems, the asymmetry between prolate and oblate models is undesirable when we restrict ourselves to axisymmetric systems. By abandoning the convention that $c < a$, our present definition of spheroidal coordinates avoids this asymmetry. For $a > c$ we have prolate spheroidal coordinates, and their definition coincides with the one given in Z85. For $a < c$ the coordinates are oblate spheroidal, and the above formulae can be transformed into those given in Z85 by the substitutions $\nu \rightarrow \mu, a \rightarrow b, c \rightarrow a, z \rightarrow x$, and $\varpi \rightarrow \bar{z}$. As a result, the symmetry axis is always the z -axis.

b) Stäckel Models

Consider an axisymmetric mass model with density distribution ρ . Let ψ be minus its gravitational potential V . This model is a Stäckel model if there is a spheroidal coordinate system (λ, ϕ, ν) in which ψ can be written as

$$\psi(\lambda, \nu) = \frac{(\lambda + \gamma)G(\lambda) - (\nu + \gamma)G(\nu)}{\lambda - \nu}, \quad (2.5)$$

where $G(\tau)$ is an arbitrary function. For a model with a finite total mass M we require that $\psi \rightarrow 0$ at large radii. This means that $G(\lambda) \sim GM/(\lambda)^{1/2}$ for $\lambda \rightarrow \infty$, where G is the gravitational constant.

The density $\rho(\lambda, \nu)$ —defined such that $\rho dx dy dz$ is the mass in the volume element $dx dy dz$ —that corresponds to a Stäckel potential can be calculated by means of the Kuzmin Formula (Kuzmin 1956; de Zeeuw 1985b), or directly from the Poisson equation:

$$\pi G(\nu - \lambda)\rho(\lambda, \nu) = (\lambda + \alpha)(\lambda + \gamma) \frac{\partial^2 \psi}{\partial \lambda^2} + \left(\frac{3}{2}\lambda + \frac{1}{2}\alpha + \gamma\right) \frac{\partial \psi}{\partial \lambda} - (\nu + \alpha)(\nu + \gamma) \frac{\partial^2 \psi}{\partial \nu^2} - \left(\frac{3}{2}\nu + \frac{1}{2}\alpha + \gamma\right) \frac{\partial \psi}{\partial \nu}. \quad (2.6)$$

Models with a Stäckel potential in prolate spheroidal coordinates generally—but not always—lead to mass models with an oblate density distribution, and vice versa (Eddington 1915*b*; de Zeeuw, Peletier, and Franx 1986). When we consider the “oblate case” and the “prolate case” in the sequel, we always refer to the shape of the density contours.

Contrary to the convention of Z85, here and below we prefer to work with ψ rather than V . This is customary in the construction of equilibrium models, and simplifies the interpretation of the equations by virtue of the fact that $\psi \geq 0$. From now on, we shall simply refer to ψ as the potential.

c) Equations of Motion

The Hamiltonian H per unit mass for motion in the potential $\psi(\lambda, \nu)$ is

$$H = \frac{p_\lambda^2}{2P^2} + \frac{p_\phi^2}{2\varpi^2} + \frac{p_\nu^2}{2R^2} - \psi(\lambda, \nu), \quad (2.7)$$

where P and R are the metric coefficients of the spheroidal coordinates, given by

$$P^2 = \frac{(\lambda - \nu)}{4(\lambda + \alpha)(\lambda + \gamma)}, \quad R^2 = \frac{(\nu - \lambda)}{4(\nu + \alpha)(\nu + \gamma)}, \quad (2.8)$$

and

$$p_\lambda = P^2 \dot{\lambda} = P v_\lambda, \quad p_\phi = \varpi^2 \dot{\phi} = \varpi v_\phi, \quad p_\nu = R^2 \dot{\nu} = R v_\nu, \quad (2.9)$$

are the momenta conjugate to λ , ϕ , and ν . It is evident that p_ϕ is equal to the component of the angular momentum L_z along the symmetry axis. The velocities v_λ , v_ϕ , and v_ν at a point (λ, ϕ, ν) are the components of the velocity \mathbf{v} along the orthogonal axes defined locally by the spheroidal coordinate system. The transformation formula from (v_λ, v_ν) to (v_ϖ, v_z) is easily derived by means of equations (2.1), (2.8), and (2.9):

$$\begin{pmatrix} v_\varpi \\ \text{sign}(z)v_z \end{pmatrix} = \begin{pmatrix} \cos \Theta & -\sin \Theta \\ \sin \Theta & \cos \Theta \end{pmatrix} \begin{pmatrix} v_\lambda \\ \text{sign}(\gamma - \alpha)v_\nu \end{pmatrix}, \quad (2.10a)$$

with

$$\cos \Theta = \sqrt{\frac{(\nu + \alpha)(\lambda + \gamma)}{(\alpha - \gamma)(\lambda - \nu)}}, \quad \sin \Theta = \sqrt{\frac{(\lambda + \alpha)(\nu + \gamma)}{(\gamma - \alpha)(\lambda - \nu)}}. \quad (2.10b)$$

Here Θ is the angle of the v_λ -axis with respect to the v_ϖ -axis, measured clockwise if $z > 0$ and counterclockwise if $z < 0$. At the foci, $\lambda = \nu = -\alpha$, and Θ is indeterminate. This is a consequence of the fact that the foci are the singular points of the coordinate system. We can already infer from this that at the foci every nonsingular velocity distribution will be isotropic in v_λ and v_ν .

The equations of motion can be written as

$$p_\tau^2 = \frac{1}{2(\tau + \alpha)} \left[G(\tau) - \frac{I_2}{\tau + \alpha} - \frac{I_3}{\tau + \gamma} - E \right], \quad \tau = \lambda, \nu, \quad (2.11)$$

and

$$p_\phi^2 = L_z^2 = 2I_2. \quad (2.12)$$

The quantities E , I_2 , and I_3 are the three integrals of motion admitted by ψ . E is minus the Hamiltonian, and hence is the binding energy per unit mass, $I_2 = \frac{1}{2}L_z^2$, and I_3 is given by

$$I_3 = \frac{1}{2}(L_x^2 + L_y^2) + (\gamma - \alpha) \left[\frac{1}{2}v_z^2 - z^2 \frac{G(\lambda) - G(\nu)}{\lambda - \nu} \right], \quad (2.13)$$

a result that can be established by applying formulae (6), (13), and (16) from de Zeeuw (1985*b*) together with equation (2.5). As pointed out by de Zeeuw and Lynden-Bell (1985), I_3 can be considered as a generalization of $L^2 - L_z^2$, with L^2 the square of the total angular momentum, which is an integral of motion in the spherical limit.

d) Orbital Structure

Each combination of values of E , I_2 , and I_3 for which the expressions for p_τ^2 and p_ϕ^2 given in equations (2.11) and (2.12) are nonnegative corresponds to an orbit. It is evident that this requires $I_2 \geq 0$. Also, p_λ^2 and p_ν^2 will generally be nonnegative in limited ranges of λ and ν only, so that

$$\nu_- \leq \nu \leq \nu_+, \quad \lambda_- \leq \lambda \leq \lambda_+, \quad (2.14)$$

where the turning points ν_- , ν_+ , λ_- , and λ_+ are the values of λ and ν for which $p_\nu^2 = 0$ and $p_\lambda^2 = 0$, respectively. They are functions of E , I_2 , and I_3 . As a result, the orbit is restricted to an area in the meridional plane, and hence to a volume in space, which it generally fills up. For $I_2 > 0$ each orbit has a definite sense of rotation around the symmetry axis. Both right-handed and left-handed motion around the z -axis may occur.

It follows from the above that every orbit is represented by a point in integral space. The volume in integral space that corresponds to allowed orbits is limited by the values of E , I_2 , and I_3 for which $\nu_- = \nu_+$, or both. The corresponding orbits are confined to a surface or curve in configuration space.

A full discussion of the orbits in oblate and prolate Stäckel models can be found in Z85. Here we summarize the relevant results in the present convention. Although we treat oblate and prolate systems in the same spheroidal coordinate system, the orbital structure is not the same in the two cases, so that they have to be discussed separately.

For oblate models we have $a > c$, and it follows from equation (2.13) that $I_3 \geq 0$. All orbits are short axis tubes, characterized by

$$c^2 \leq \nu \leq \nu_+, \quad \lambda_- \leq \lambda \leq \lambda_+. \tag{2.15}$$

Thus, a short axis tube fills a volume in space that is limited by two prolate spheroids and one hyperboloid of one sheet (see Fig. 24 of Z85). Figure 1 shows the classification of bound orbits in integral space. The special orbits that occur for limiting values of the integrals are indicated.

Prolate models occur for $a < c$. In this case I_3 may have positive and negative values. Orbits with $I_3 > 0$ are outer long axis tubes, characterized by

$$\nu_- \leq \nu \leq c^2, \quad \lambda_- \leq \lambda \leq \lambda_+. \tag{2.16}$$

In general, an outer long axis tube fills a volume in space limited by two oblate spheroids and a hyperboloid of two sheets (see Z85, Fig. 20b). Orbits with $I_3 < 0$ are inner long axis tubes, and have

$$\nu_- \leq \nu \leq \nu_+, \quad c^2 \leq \lambda \leq \lambda_+. \tag{2.17}$$

Inner long axis tubes fill a volume in space limited by one oblate spheroid and two hyperboloids of one sheet (Z85, Fig. 20a). The integral space for prolate models is presented in Figure 2.

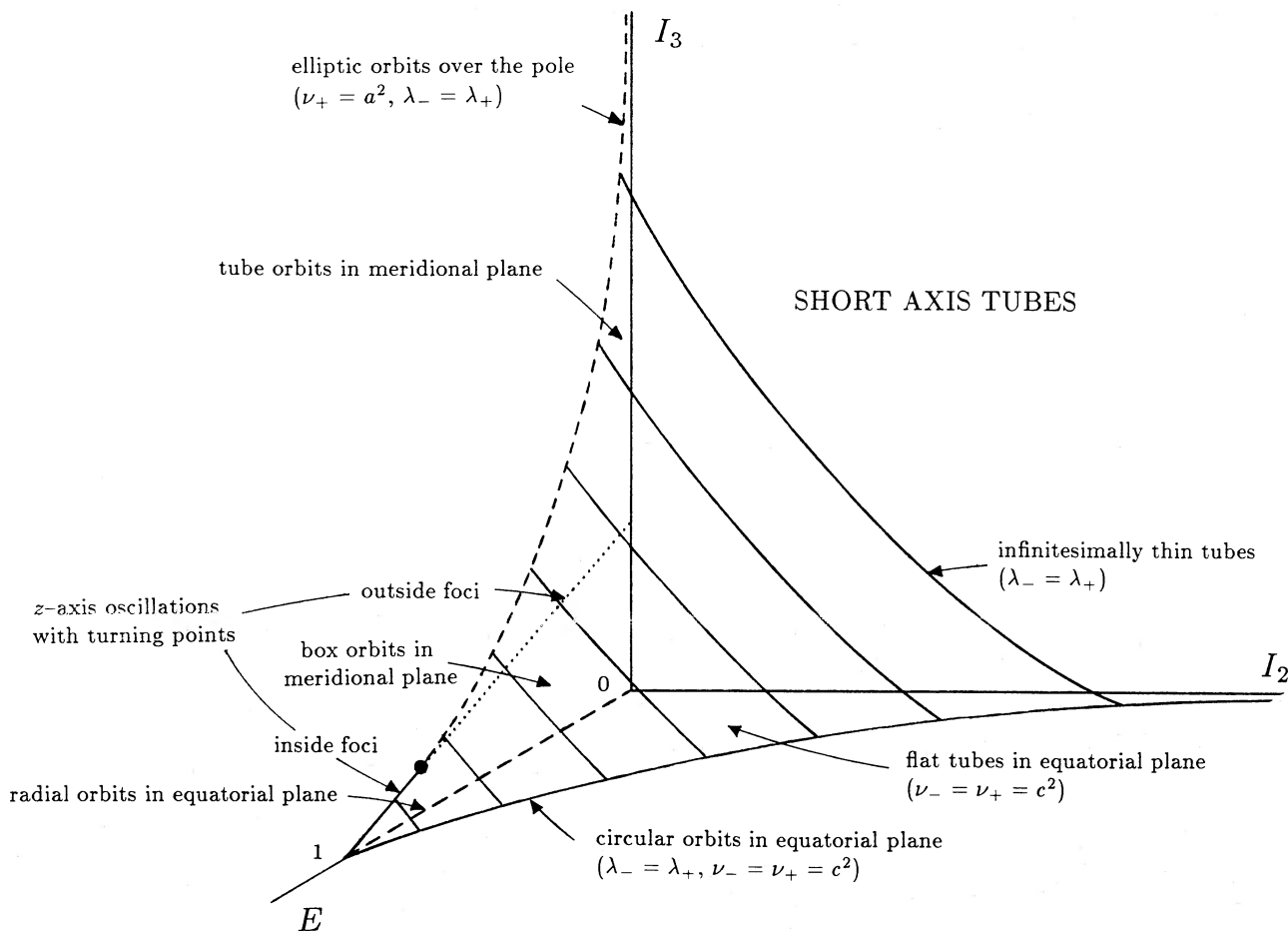


FIG. 1.—Three-dimensional integral space (E, I_2, I_3) for oblate Stäckel models ($c < a$). Each point within the volume shown corresponds to a bound orbit. Dashed and dotted lines represent periodic orbits that are unstable in one, respectively two, directions. The filled circle corresponds to the z -axis oscillation that just reaches the foci.

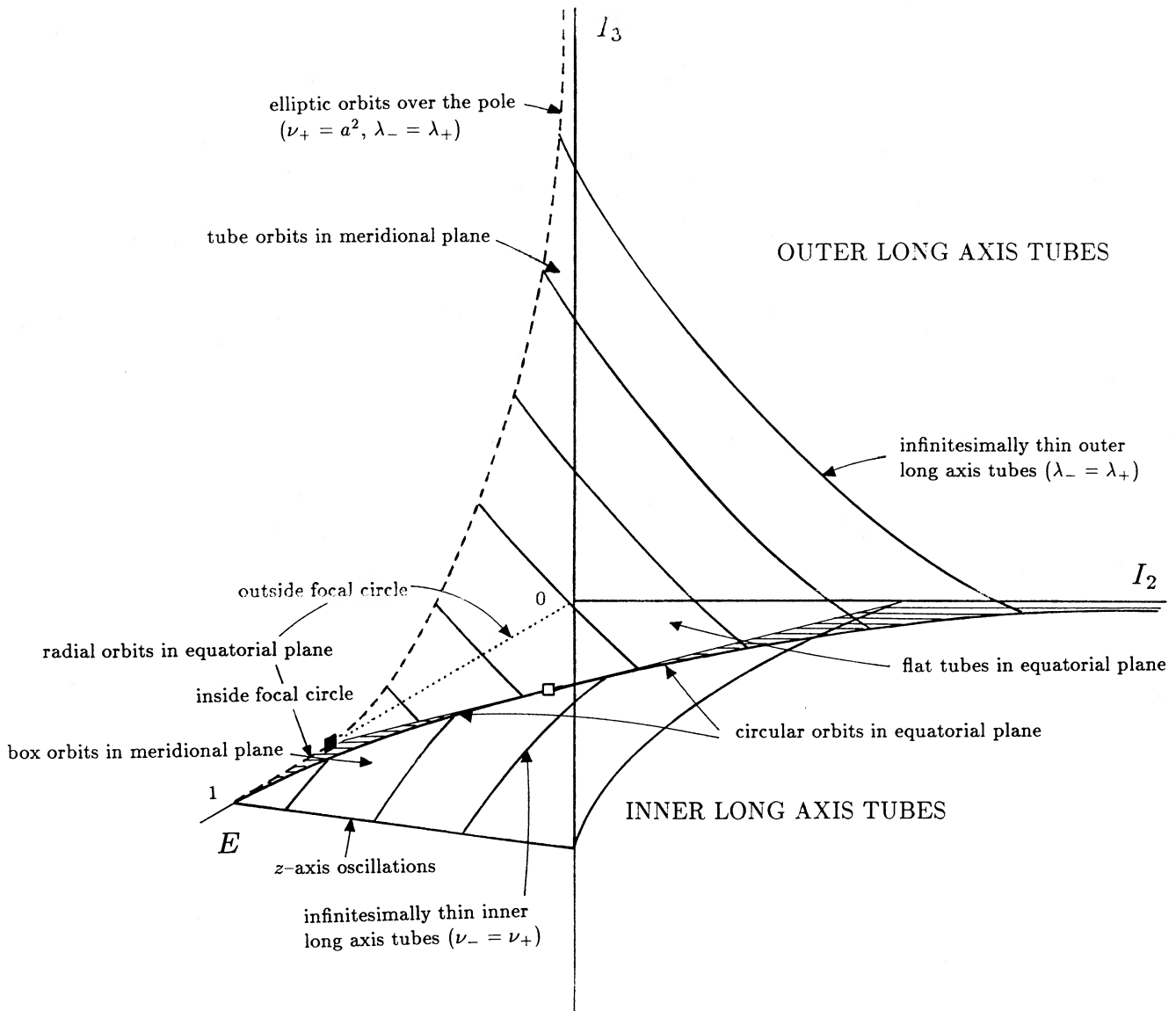


FIG. 2.—As Fig. 1, but for prolate Stäckel models ($c > a$). Open square corresponds to the circular orbit that coincides with the focal circle. Filled square is the radial orbit in the equatorial plane that just reaches the focal circle. Stable flat tube orbits in the equatorial plane occur only in the hatched areas.

III. DISTRIBUTION FUNCTIONS

a) Fundamental Integral Equation

Let F be the distribution function, defined in the usual way as a probability density in phase space and in canonical coordinates. F is related to the mass density by the fundamental integral equation

$$\rho(\varpi, z) = \iiint F(\varpi, z, v_\varpi, v_\phi, v_z) dv_\varpi dv_\phi dv_z, \tag{3.1}$$

where the integration extends over all possible velocities. In a Stäckel model all orbits admit three exact isolating integrals of motion, E , L_z , and I_3 , so that Jeans's (1915) theorem applies, and $F = F(E, L_z, I_3)$. Since L_z is an odd function of v_ϕ it follows that F , considered as a function of L_z for fixed E and I_3 , can generally be written as the sum of an even and an odd part. The odd part has no impact on the density distribution, but determines how many stars are orbiting right-handed ($L_z > 0$) and left-handed ($L_z < 0$). There are two extreme cases:

1. The fraction of right-handed stars is equal to the fraction of left-handed stars. In this case the odd part of F is zero and there is no net rotation around the z -axis. We shall denote the corresponding distribution function by $F(E, I_2, I_3)$, where $2I_2 = L_z^2$.
2. Only right-handed (or left-handed) stars occur. Now there is a maximum amount of rotation for the given form of the even part of F . In this case we write the distribution function as $F^+(E, I_2, I_3)$ [or $F^-(E, I_2, I_3)$].

First consider the case of no net rotation. Upon transformation from the variables v_ϖ , v_ϕ , and v_z to E , I_2 , and I_3 by means of equations (2.9), (2.11), (2.12), and (2.13) the fundamental integral equation can be written as (see also Z85)

$$\rho(\varpi, z) = \frac{2\sqrt{2}}{\varpi} \iiint \frac{F(E, I_2, I_3)}{\sqrt{(\lambda + \gamma)N(\lambda)}\sqrt{-(v + \gamma)N(v)}\sqrt{I_2}} dE dI_2 dI_3, \quad (3.2)$$

with

$$N(\tau) = G(\tau) - E - \frac{I_2}{\tau + \alpha} - \frac{I_3}{\tau + \gamma}. \quad (3.3)$$

The integrations extend over all values of E , I_2 , and I_3 for which $p_\lambda^2 \geq 0$, $p_\phi^2 \geq 0$, and $p_v^2 \geq 0$, so that the arguments of the square roots in equation (3.2) are nonnegative.

The boundaries of the integration volume in the (E, I_2, I_3) -space follow from the conditions $p_\lambda^2 = 0$, $p_\phi^2 = 0$, and $p_v^2 = 0$. We find

$$\begin{aligned} p_\lambda^2 = 0 &\Leftrightarrow I_3 = I_3^+(E, I_2, \lambda) = (\lambda + \gamma)[G(\lambda) - E] - \frac{\lambda + \gamma}{\lambda + \alpha} I_2, \\ p_\phi^2 = 0 &\Leftrightarrow I_2 = 0, \\ p_v^2 = 0 &\Leftrightarrow I_3 = I_3^-(E, I_2, v) = (v + \gamma)[G(v) - E] + \frac{v + \gamma}{v + \alpha} I_2, \end{aligned} \quad (3.4)$$

so that the volume is bounded by planes. Figures 3a and 3b show the (I_2, I_3) -plane for a constant value of E , for the oblate and prolate cases, respectively. For a given point (λ, v) , or (ϖ, z) , the integrations over I_2 and I_3 are over the triangular region bounded by the straight lines which are the intersection of the planes defined in equation (3.4) with a surface of constant E . All values of I_2 and I_3 inside the triangle correspond to orbits that pass through the point (λ, v) for this value of E . Thus, the integration over I_3 is between the values I_3^- and I_3^+ . It follows that the integration over I_2 runs between 0 and the value I_2^+ for which the two straight lines intersect, i.e., for which $I_3^+ = I_3^-$. We find

$$I_2^+ = I_2^+(E, \lambda, v) = \frac{(\lambda + \alpha)(v + \alpha)}{\alpha - \gamma} (\psi - E) = \varpi^2(\psi - E). \quad (3.5)$$

This expression shows immediately that the E -integration is over values between 0 and ψ . This is in agreement with the fact that the orbit with lowest energy that passes through (λ, v) is the one with turning points in both λ and v there, so that $E = \psi(\lambda, v)$. As a result, the fundamental integral equation is

$$\rho(\varpi, z) = \frac{2\sqrt{2}}{\varpi} \int_0^\psi dE \int_0^{I_2^+(E, \lambda, v)} \frac{dI_2}{\sqrt{I_2}} \int_{I_3^-(E, I_2, v)}^{I_3^+(E, I_2, \lambda)} \frac{F(E, I_2, I_3) dI_3}{\sqrt{I_3^+(E, I_2, \lambda) - I_3} \sqrt{I_3 - I_3^-(E, I_2, v)}}. \quad (3.6)$$

In the special case where the distribution function does not depend on the third integral, the integration over I_3 can be done immediately, and we find

$$\rho(\varpi, z) = \frac{2\pi\sqrt{2}}{\varpi} \int_0^\psi dE \int_0^{I_2^+} F(E, I_2) \frac{dI_2}{\sqrt{I_2}}, \quad (3.7)$$

or, equivalently,

$$\rho(\varpi, z) = 4\pi \int_0^\psi dE \int_0^{\sqrt{2(\psi - E)}} F(E, L_z) dv_\phi, \quad (3.8)$$

which is the well-known result (e.g., D86, eq. [2.2.19]).

In the second case mentioned earlier, where only right-handed (or left-handed) stars occur, the fundamental integral equation (3.6) becomes

$$\rho^\pm(\varpi, z) = \frac{\sqrt{2}}{\varpi} \int_0^\psi dE \int_0^{I_2^+(E, \lambda, v)} \frac{dI_2}{\sqrt{I_2}} \int_{I_3^-(E, I_2, v)}^{I_3^+(E, I_2, \lambda)} \frac{F^\pm(E, I_2, I_3) dI_3}{\sqrt{I_3^+(E, I_2, \lambda) - I_3} \sqrt{I_3 - I_3^-(E, I_2, v)}}. \quad (3.9)$$

When F^\pm depends on E and L_z only we obtain

$$\rho^\pm(\varpi, z) = 2\pi \int_0^\psi dE \int_0^{\sqrt{2(\psi - E)}} F^\pm(E, L_z) dv_\phi. \quad (3.10)$$

For a given density $\rho(\varpi, z)$ and potential $\psi(\varpi, z)$, equation (3.6) is an integral equation for $F(E, I_2, I_3)$. Since F depends on three arguments, and ρ on only two, it is to be expected that generally many solutions exist. Indeed, it is well known that, even if F is restricted to depend on E and I_2 only, a solution exists (see also § IIIb). A solution F is physical when $F \geq 0$. Such a distribution function is said to be consistent with the density ρ in the given potential ψ . In the special case where ψ is the gravitational potential of the density ρ itself—so that ρ and ψ are connected via Poisson's equation— F , ρ , and ψ describe a self-consistent dynamical model.

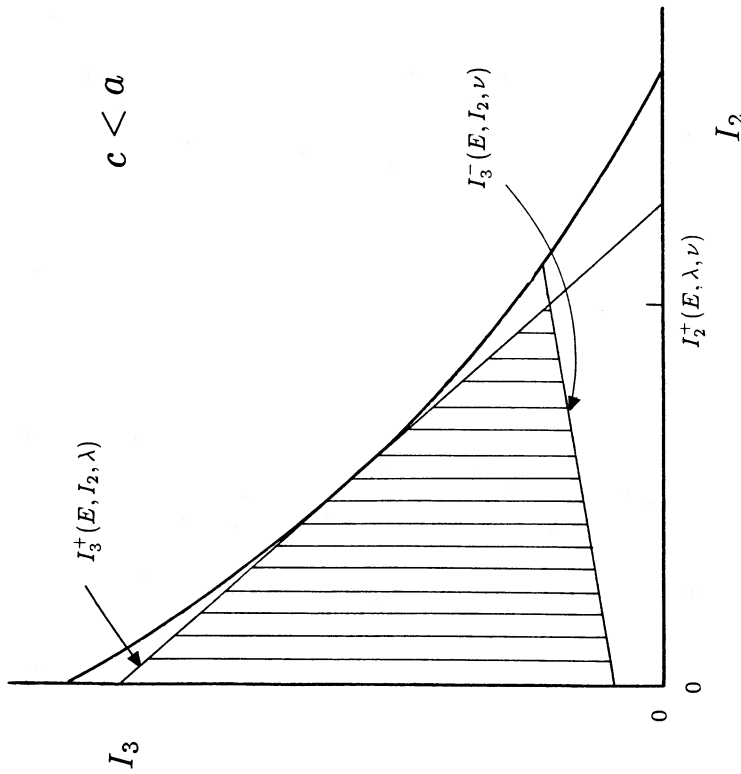
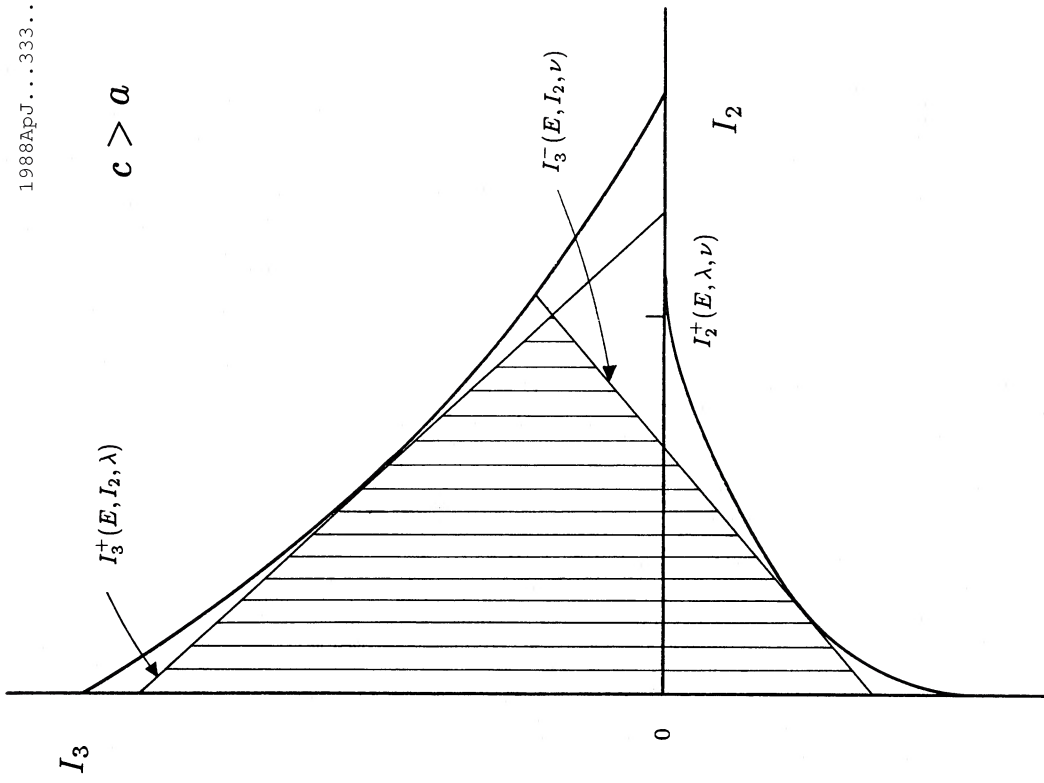


FIG. 3.—Planes of constant energy E for oblate and prolate Stäckel models. Shaded area indicates all orbits which pass through a given point (λ, ν) , and is the region of integration for eq. (3.6).

Instead of using E , I_2 , and I_3 as arguments of F , we could also have employed the turning points of the individual orbits as integrals of motion. This approach was taken by Bishop (1986) and Statler (1987). It is particularly useful for the study of Stäckel models in which only infinitesimally thin tube orbits occur (Bishop 1987; de Zeeuw 1988). In the prolate case one has to distinguish between inner and outer long axis tubes, and hence one must solve a separate integral equation for each orbit family (Hunter *et al.* 1988).

b) Construction of Distribution Functions

Finding solutions of the fundamental integral equation (3.6) is not an easy task. It is useful to consider briefly the simpler problem of solving equation (3.8) for a function $F(E, I_2)$.

Fricke (1952) expressed the two-integral distribution function as a double series of the form

$$F(E, I_2) = \sum_{l, m} a_{lm} E^l I_2^m, \quad (3.11)$$

where l and m may take any real values, and he showed that this corresponds to a density distribution ρ that is given by

$$\rho(\varpi, z) = 2\pi \sum_{l, m} a_{lm} \frac{\Gamma(l+1)\Gamma(m+1/2)}{\Gamma(l+m+1/2)} \varpi^{2m} \psi^{l+m+3/2}. \quad (3.12)$$

If a given density $\rho(\varpi, z)$ in a potential $\psi(\varpi, z)$ can be expressed as $\rho(\varpi, \psi)$, and can be expanded in the form (3.12), then the unique distribution function $F(E, I_2)$ that is consistent with it follows immediately from equation (3.11). However, the convergence of the resulting series expansion for $F(E, I_2)$ is not guaranteed for all values of E and I_2 .

Since 1952, more powerful inversion techniques have been developed that give F once $\rho = \rho(\varpi, \psi)$ is known. Lynden-Bell (1962) formulated the problem in terms of inverse Laplace transforms. Hunter (1975b) employed Stieltjes transforms, while D86 used Mellin transforms (see also Kalnajs 1976). Expression of ρ as $\rho(\varpi, \psi)$ is easy enough numerically, but it strongly limits the possible potentials if results are to be obtained in a mathematically explicit form. This is effectively a requirement, since it can be shown that the two-integral inversion problem is badly posed in the Hadamard sense, and involves an analytic continuation which is numerically unstable (D86). As a result, to date only a small number of exact axisymmetric models with $F = F(E, I_2)$ have been constructed (for a review, see Hunter 1975a; de Zeeuw 1987). In nearly all these cases the distribution function $F(E, I_2)$ can in fact be found by Fricke's method. The advantage of the more powerful inversion techniques is that either they give F in a form that is convergent for all values of E and I_2 , or they allow more possibilities to obtain convergent representations in cases for which the convergence of the "naive" power series is slow, or breaks down. We will encounter an example of this in § IVc.

It follows from the above that it should be useful to extend Fricke's approach to distribution functions that depend on three integrals. Accordingly, we write

$$F(E, I_2, I_3) = \sum_{l, m, n} a_{lmn} E^l I_2^m (I_2 + I_3)^n, \quad (3.13)$$

where l and m may take real values, but n is an integer. The simplest generalization of expression (3.11) would be to expand in terms of powers of I_3 . However, taking powers of $I_2 + I_3$ does not complicate the resulting calculations substantially, and has the advantage that the individual components reduce to simple forms in the spherical limit, since then $I_2 + I_3 \rightarrow \frac{1}{2}L^2$ (see § IIIe below).

In Appendix A we give the derivation of the density distribution that corresponds to the distribution function of equation (3.13), as calculated by direct evaluation of the integral (3.6). There we consider a form for the individual components which is slightly more general than the one given in equation (3.13), with powers of $(p + qE + rI_2 + 2sI_3)$ instead of powers of $(I_2 + I_3)$ as the third factor. Substitution of $p = q = 0$, $r = 1$, and $s = \frac{1}{2}$ in equation (A15) gives, after some rearrangement of terms,

$$\rho(\lambda, v) = \sum_{l, m, n} a_{lmn} \rho_{lmn}(\lambda, v), \quad (3.14)$$

where an individual density component is given by

$$\begin{aligned} \rho_{lmn}(\lambda, v) = & 2^{3/2-n} \sqrt{\pi n!} \Gamma(l+1) \varpi^{2m} \psi^{l+m+3/2} \sum_{k=0}^n \frac{1}{\Gamma(3/2+m+k)} \sum_{i=0}^{k/2} \frac{\Gamma(i+1/2)\Gamma(1/2+m+k-2i)}{i!(k-2i)!} (\lambda-v)^{2i} (\lambda+v+2\alpha)^{k-2i} \\ & \times \sum_{j=0}^{n-k} \frac{\Gamma(n+m+3/2-j)}{\Gamma(l+m+n+5/2-j)j!(n-k-j)!} (\lambda+v+2\gamma)^{n-j-k} \psi^{n-j} [2\gamma(U-\psi)]^j, \end{aligned} \quad (3.15)$$

with

$$U = \frac{1}{c^2} \frac{v(\lambda+\gamma)G(\lambda) - \lambda(v+\gamma)G(v)}{\lambda-v}. \quad (3.16)$$

This result is valid for arbitrary axisymmetric Stäckel potentials, i.e., for an arbitrary function $G(\tau)$. It is not difficult to show that for $n = 0$ the expression (3.14) reduces to the one given in equation (3.12).

In order for ρ to correspond to a model with finite total mass, each density component ρ_{lmn} must fall off with increasing λ more rapidly than $\lambda^{-3/2}$, since $\lambda \sim r^2$ for large radii r . Inspection of equations (3.15) and (3.16) shows that this will be the case for all indices l, m , and n that satisfy the constraint

$$l - m - n > \frac{3}{2}. \quad (3.17)$$

If we can express a given density $\rho(\lambda, v)$ in a potential $\psi(\lambda, v)$ as a series of the form (3.14), then the distribution function $F(E, I_2, I_3)$ that is consistent with ρ follows immediately from equation (3.13). Moreover, each choice of such a series for ρ will give a different distribution function. In principle, this approach produces self-consistent dynamical models with a distribution function that depends on three integrals of motion, although the convergence of the resulting series for $F(E, I_2, I_3)$ is not guaranteed. However, we have little hope that the required series expansion for ρ can be found in practice. This is evident not only from the cumbersome expression (3.15) for the individual terms, but also from the fact that even for $n = 0$ only a small number of explicit cases are known.

One might wonder whether progress can be made by taking special terms in the series (3.13). An obvious choice is to take $l = m = 0$ in the more general expression for F considered in Appendix A, so that we are left with a distribution function $F = F(Q)$, where Q is a linear combination of the three integrals of motion. Distribution functions of this kind obey the generalized ellipsoidal hypothesis, and have played an important role in Galactic dynamics (e.g., Chandrasekhar 1942). However, as Eddington (1915a), Camm (1941), and Fricke (1952) showed, they lead to self-consistent models only in the spherical limit (Eddington 1914; Osipkov 1979; Merritt 1985). Dejonghe (1988) gives explicit expressions for the density that corresponds to a general $F(Q)$, and shows that distribution functions of this kind may be used to define simple density components in a given potential.

A different approach was proposed recently by Bertin and Stiavelli (1984) and Stiavelli and Bertin (1985; see also Tremaine 1987). These authors considered a distribution function of the form

$$F(E, I_2, I_3) = E^l e^{-(p+qE+rI_2+2sI_3)}, \quad (3.18)$$

where $l = 3/2$ and p, q, r , and s are constants, and they derived some properties of the corresponding model in the approximation where the departure from sphericity is small. This F can be expanded as

$$F(E, I_2, I_3) = E^l \sum_{n=0}^{\infty} \frac{(-1)^n}{n!} (p + qE + rI_2 + 2sI_3)^n, \quad (3.19)$$

which is of the form (3.13). From a computational point of view, this series expansion is formal, since equation (3.17) shows that many of the individual density components ρ_{l_0n} have infinite mass. Thus, the density distribution must be calculated directly from the fundamental integral equation (3.6). Whether the parameters in expression (3.18) can be chosen in such a way that ρ and ψ satisfy the Poisson equation, so that a self-consistent model is obtained, remains to be seen.

For the construction of exact solutions, we follow an alternative route. This is based on the observation that we are able, at least in principle, to invert equation (3.8). Moreover, two-integral models can generate the full set of axisymmetric mass densities $\rho(\varpi, z)$, although admittedly not all distribution functions will be positive definite. Therefore, there is no real mathematical restriction on the mass densities that are generated by two-integral dynamics. This means that if we decompose a given density distribution—which is assumed to follow from a prescription of the potential—into two terms

$$\rho(\lambda, v) = \rho_1(\varpi, \psi) + \rho_2(\lambda, v), \quad (3.20)$$

such that for the corresponding distribution functions the relation

$$F(E, I_2, I_3) = F_1(E, L_2^2) + F_2(E, I_2, I_3), \quad (3.21)$$

holds, then we can in principle choose F_2 freely and find ρ_2 by “straightforward” evaluation of the integral (3.6). The residual density ρ_1 then follows from equation (3.20):

$$\rho_1(\varpi, \psi) = \rho(\lambda, v) - \rho_2(\lambda, v), \quad (3.22)$$

and F_1 can be determined by one of the two-integral inversion methods mentioned earlier. The final distribution function follows from equation (3.21).

In practice, two difficulties ask for much of one’s mathematical wit. First, the integration (3.6) rapidly becomes unwieldy, especially for functions F_2 that depend on three arguments. Three argument functions are not really a requirement though, since it suffices that one argument of F_2 depends on I_3 to make F truly dependent on the three integrals. For possible one-argument functions, see Dejonghe (1988).

Three argument functions generally make ρ_2 not only cumbersome, but worse, often only expressible in terms of higher transcendental functions. This leads us to the second stumbling block: as we have seen, application of the two-integral inversion methods requires that ρ_1 is known explicitly as $\rho_1(\varpi, \psi)$. This means that we need both ρ and ρ_2 as explicit functions of ϖ and ψ . *This last requirement limits the choices of F_2 and ψ considerably.* Although one might think that this procedure is doomed to fail, we shall show in § IV that by choosing F_2 to be a finite sum of the form (3.13) exact solutions may indeed be found.

c) Kinematic Properties

We define the velocity moments $\mu_{\rho, \sigma, \tau}$ of a distribution function $F(E, I_2, I_3)$ by

$$\mu_{\rho, \sigma, \tau}(\lambda, v) = \rho \langle v_\lambda^\rho v_\phi^\sigma v_v^\tau \rangle = \iiint v_\lambda^\rho v_\phi^\sigma v_v^\tau F(E, I_2, I_3) dv_\lambda dv_\phi dv_v, \quad (3.23)$$

where the indices ρ, σ , and τ are nonnegative integers, and the integration is over all physical values of the velocities. By use of the relations (see eqs. [2.9], [2.12], and [3.4])

$$v_\lambda = \pm \frac{\sqrt{2(I_3^+ - I_3)}}{\sqrt{\lambda - v}}, \quad v_\phi = \pm \frac{\sqrt{2I_2}}{\varpi}, \quad v_v = \pm \frac{\sqrt{2(I_3 - I_3^-)}}{\sqrt{\lambda - v}}, \quad (3.24)$$

equation (3.23) can be rewritten as a triple integral over E , I_2 , and I_3 , in a form very similar to the integral (3.6). By symmetry, it follows immediately that

$$\mu_{2\rho+1,\sigma,\tau} = \mu_{\rho,\sigma,2\tau+1} = 0. \quad (3.25)$$

The nontrivial moments corresponding to a distribution function of the form $E^l I_2^m (p + qE + rI_2 + 2sI_3)^n$ can be calculated explicitly. The derivation is given in Appendix B.

The first-order moments give the components of the mean streaming velocity. We have

$$\langle v_\lambda \rangle = \langle v_\nu \rangle = 0, \quad (3.26)$$

so that also $\langle v_\omega \rangle = \langle v_z \rangle = 0$. Since every orbit has a fixed sense of rotation around the z -axis, generally $\langle v_\phi \rangle \neq 0$. As discussed in § IIIa, the extreme cases are $\langle v_\phi \rangle = 0$ and $|\langle v_\phi \rangle|$ equal to a maximum value, denoted by $\langle v_\phi^\pm \rangle$. It is given by

$$\rho \langle v_\phi^\pm \rangle = \mu_{0,1,0}. \quad (3.27)$$

In order to characterize a rotational state of the model one has to specify the fraction of right-handed stars in each orbit. Thus, there is a very large number of possibilities. One approach for bringing some order in these is to use an entropy argument. It can be shown that the total z -component of the angular momentum, $L_{z,T}$, can be used to parametrize the most probable—in the Jaynes sense—rotational state (Dejonghe 1987). Its distribution function is given by

$$F_\zeta(E, L_z, I_3) = \frac{2F(E, I_2, I_3)}{1 + e^{-\zeta L_z}}, \quad (3.28)$$

where as usual F is the even part of F_ζ , i.e., the solution for zero streaming. The value of the parameter ζ determines the total angular momentum $L_{z,T}$. Unfortunately, due to the exponential in the denominator of the expression for F_ζ , it is cumbersome to derive the odd velocity moments of the model with the most probable rotational state in closed form. For that reason we limit ourselves to the two extreme cases defined in § IIIa.

The second-order moments are related to the velocity dispersions. For the mixed moments we have

$$\langle v_\lambda v_\phi \rangle = \langle v_\lambda v_\nu \rangle = \langle v_\phi v_\nu \rangle = 0. \quad (3.29)$$

This shows that in a Stäckel model the principal axes of the velocity ellipsoid are always aligned with the spheroidal coordinates in which the potential is of Stäckel form, a result first proven by Eddington (1915b). The three principal velocity dispersions are given by

$$\rho \sigma_\lambda^2 = \mu_{2,0,0}, \quad \rho[\sigma_\phi^2 + \langle v_\phi \rangle^2] = \mu_{0,2,0}, \quad \rho \sigma_\nu^2 = \mu_{0,0,2}. \quad (3.30)$$

In the cylindrical coordinates (ϖ, ϕ, z) we find, by means of equation (2.10),

$$\begin{aligned} \rho \sigma_\omega^2 = \langle v_\omega^2 \rangle &= \sigma_\lambda^2 \cos^2 \Theta + \sigma_\nu^2 \sin^2 \Theta, & \rho \sigma_{\omega z}^2 = \langle v_\omega v_z \rangle &= \frac{1}{2} \text{sign}(z)(\sigma_\lambda^2 - \sigma_\nu^2) \sin 2\Theta, \\ \rho \sigma_z^2 = \langle v_z^2 \rangle &= \sigma_\lambda^2 \sin^2 \Theta + \sigma_\nu^2 \cos^2 \Theta. \end{aligned} \quad (3.31)$$

For the special case where $F = F(E, I_2)$, the dispersions can be expressed directly in terms of ρ and ψ as follows (Hunter 1977; D86, eqs. [2.3.10], [2.3.11]):

$$\rho \sigma_\omega^2 = \rho \sigma_z^2 = \frac{1}{2} \mu_{2,0} = \int_0^\psi \rho(\varpi, \psi') d\psi', \quad \rho[\sigma_\phi^2 + \langle v_\phi \rangle^2] = \mu_{0,2} = \int_0^\psi \frac{\partial}{\partial \varpi} [\varpi \rho(\varpi, \psi')] d\psi'. \quad (3.32)$$

A similar explicit expression can be derived for $\langle v_\phi^\pm \rangle$. It is given by (D86, eq. [2.3.9])

$$\rho \langle v_\phi^\pm \rangle = \mu_{0,1} = \pm \frac{\sqrt{2}}{\pi} \int_0^\psi \frac{d\psi'}{\sqrt{\psi - \psi'}} \frac{\partial}{\partial \varpi} \int_0^\varpi \omega' \rho^\pm(\omega', \psi') \frac{d\omega'}{\sqrt{\omega'^2 - \varpi'^2}}. \quad (3.33)$$

In the above equations $\mu_{2,0}$, $\mu_{0,2}$, and $\mu_{0,1}$ are identical to the simplified moments defined in Appendix C.

The second-order moments of the distribution function are related to ρ and ψ by the Jeans equations. For axisymmetric Stäckel models, these were written down first by Lynden-Bell (1960). Evans and Lynden-Bell (1988) have studied solutions of the Jeans equations by means of Green's function methods. As we have shown by construction in § IIIb, generally many different distribution functions $F(E, I_2, I_3)$ are consistent with a given ρ , so that the Jeans equations alone do not fix all three second-order moments. By analogy with the work of Bacon (1985), we show in Appendix D that for a given ρ and ψ of axisymmetric Stäckel form, the Jeans equations uniquely determine $\langle v_\lambda^2 \rangle$, $\langle v_\phi^2 \rangle$, and $\langle v_\nu^2 \rangle$, once the ratio of $\langle v_\phi^2 \rangle$ and $\langle v_\nu^2 \rangle$ has been specified in the complete meridional plane. The special case where $\langle v_\lambda^2 \rangle = \langle v_\nu^2 \rangle$ everywhere leads to the well-known solution (3.32) for the model with $F = F(E, I_2)$.

Unfortunately, positive definite solutions of the Jeans equations do not necessarily guarantee a positive distribution function. From the point of view of a rigorous analysis, this is a major drawback, as it remains necessary to construct a distribution function in order to check its sign.

d) Spherical Limit

In the special case where $c = a$ the spheroidal coordinates reduce to spherical coordinates (see § IIa), and the models become spherical. In this limit the distribution function F is given by

$$F = \sum_{l,m,n} a_{lmn} 2^{-m-n} E^l L_z^m L^2 n, \quad (3.34)$$

and the corresponding density follows from equation (3.14) upon taking $\gamma = \alpha$, $\nu = -\alpha$, and $\lambda + \alpha = r^2$. An individual density component is given by

$$\rho_{lmn} = 2^{3/2-n} \sqrt{\pi n!} \Gamma(l+1) \frac{\Gamma(n+m+3/2)}{\Gamma(l+m+n+5/2)} \varpi^{2m} r^{2n} \psi^{l+m+n+3/2} \sum_{k=0}^n \frac{1}{(n-k)! \Gamma(m+k+3/2)} \sum_{i=0}^{k/2} \frac{\Gamma(i+1/2) \Gamma(m+k-2i+1/2)}{i!(k-2i)!}. \quad (3.35)$$

By means of techniques similar to those employed in Appendix A, we find that the double summation can be performed explicitly. We are left with

$$\rho_{lmn} = 2^{3/2} \pi \frac{\Gamma(l+1) \Gamma(m+1/2) \Gamma(m+n+1)}{\Gamma(m+1) \Gamma(l+m+n+5/2)} \varpi^{2m} r^{2n} \psi^{l+m+n+3/2}. \quad (3.36)$$

For $m = 0$ this reduces to the result obtained by D86 (eq. [1.7.12]). Distribution functions of the form (3.34) can be used to describe axisymmetric components in a spherical potential. Models of this kind were constructed by White (1985).

IV. AN EXACT MODEL

In this section we apply the method described in § IIIb to an axisymmetric mass model originally introduced by Kuzmin (1956), and subsequently studied by Kuzmin and Kutuzov (1962).

a) Mass Model

The Kuzmin-Kutuzov model has a very simple potential ψ . It is defined by the choice

$$G(\tau) = \frac{GM}{c + \sqrt{\tau}}, \quad (\tau = \lambda, \nu), \quad (4.1)$$

so that we have (see eq. [2.5])

$$\psi(\lambda, \nu) = \frac{GM}{\sqrt{\lambda} + \sqrt{\nu}}. \quad (4.2)$$

Near the center the equipotential surfaces are approximately spheroidal, with axis ratio equal to $(c/a)^{1/2}$. At larger radii the potential becomes increasingly more nearly spherical.

The density distribution that corresponds to this potential can be calculated by the methods outlined in § IIb. We obtain

$$\rho(\lambda, \nu) = \frac{Mc^2 [\lambda\nu + a^2(\lambda + 3\sqrt{\lambda\nu} + \nu)]}{4\pi (\lambda\nu)^{3/2} (\sqrt{\lambda} + \sqrt{\nu})^3}. \quad (4.3)$$

Near the center the density can be expanded in a Taylor series in ϖ and z as follows:

$$\rho(\varpi, z) = \rho_0 \left(1 - \frac{\varpi^2}{a_1^2} - \frac{z^2}{a_3^2} + \dots \right). \quad (4.4)$$

The central density ρ_0 equals $\rho(a^2, c^2)$, and is given by

$$\rho_0 = \frac{M(a+2c)}{4\pi ac(a+c)^2}. \quad (4.5)$$

The values of the semiaxes a_1 and a_3 can be found by application of equations (34) and (35) of de Zeeuw, Peletier, and Franx (1986). We obtain

$$\frac{a_1^2}{a^2} = \frac{a(a+c)(a+2c)}{2(a^2+3ac+c^2)}, \quad \xi_0^2 = \frac{a_3^2}{a_1^2} = 4 \frac{c^2}{a^2} \frac{a^2+3ac+c^2}{3a^2+9ac+8c^2}. \quad (4.6)$$

Near the center, the surfaces of constant density are approximately spheroidal. For $c < a$ the spheroids are oblate, and for $c > a$ they are prolate. At large radii the density falls off proportional to r^{-4} , and the axis ratio ξ approaches a limiting value ξ_∞ given by

$$\xi_\infty^4 = \frac{2c^3}{a(a^2+c^2)}. \quad (4.7)$$

All models become slightly more nearly spherical with increasing radius. As an example, we show in Figure 4 density contours for the cases $c/a = 0.5$ and $c/a = 1.25$. Figure 5 shows ξ as a function of the distance along the z -axis, for the same values of a and c .

The inherent conciseness of the formulation in spheroidal coordinates becomes apparent when we write the potential and density of the Kuzmin-Kutuzov model in the customary cylindrical coordinates. By means of the relations (see Z85)

$$\lambda + \nu = \varpi^2 + z^2 + a^2 + c^2, \quad \lambda\nu = a^2c^2 + c^2\varpi^2 + a^2z^2, \quad (4.8)$$

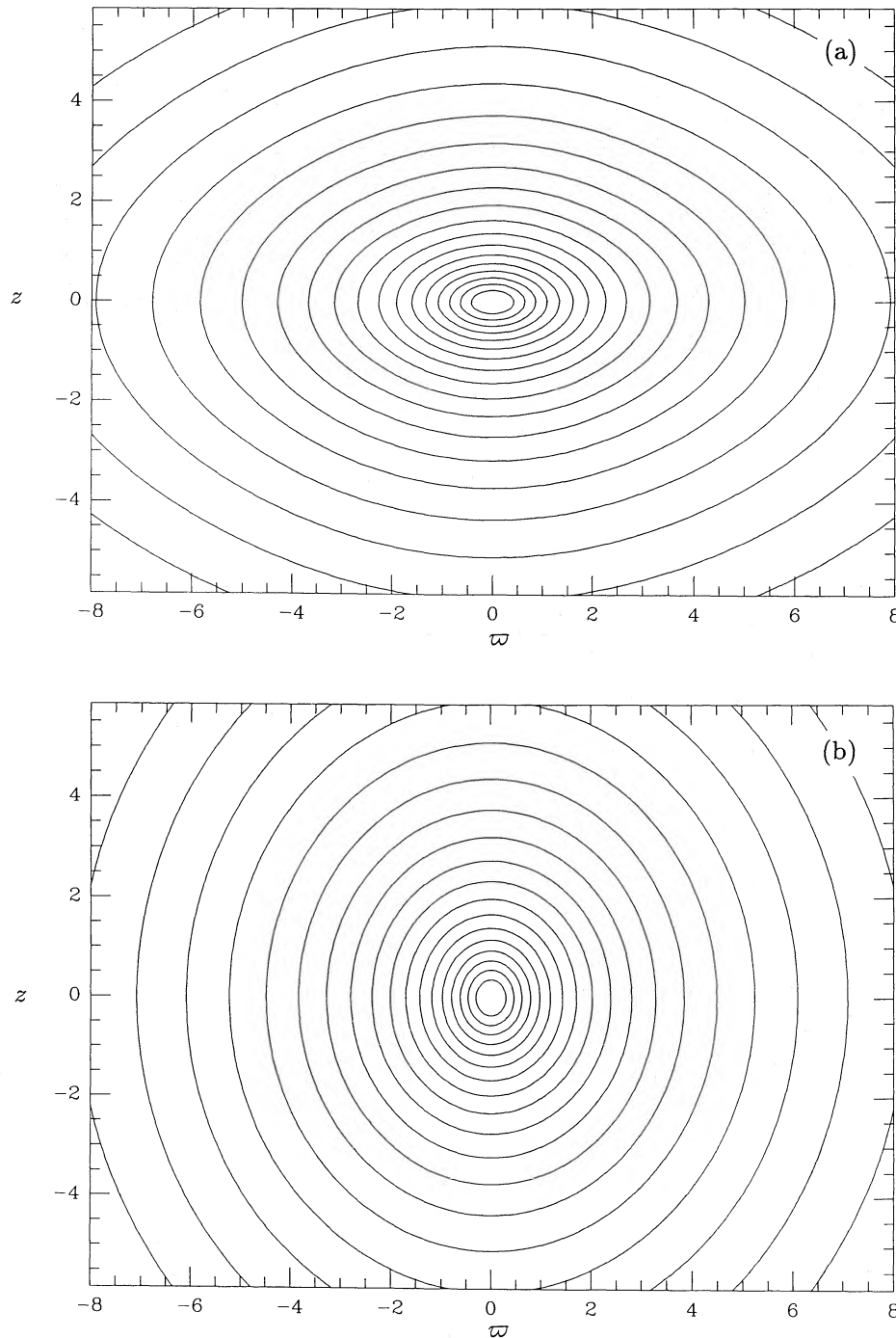


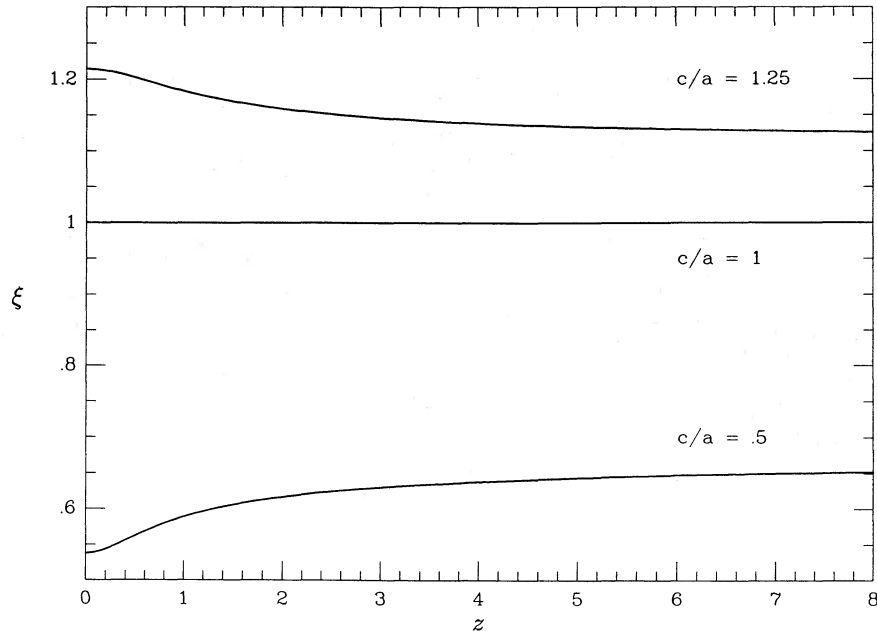
FIG. 4.—Contours of constant density in the meridional plane for the Kuzmin-Kutuzov model. The density contrast between the inner and outer contour is of the order of 10^5 . (a) $c/a = 0.5$ (b) $c/a = 1.25$.

we obtain

$$\psi(w, z) = \frac{GM}{(w^2 + z^2 + a^2 + c^2 + 2\sqrt{a^2c^2 + c^2w^2 + a^2z^2})^{1/2}} \quad (4.9)$$

and

$$\rho(w, z) = \frac{Mc^2}{4\pi} \frac{(a^2 + c^2)w^2 + 2a^2z^2 + 2a^2c^2 + a^4 + 3a^2\sqrt{a^2c^2 + c^2w^2 + a^2z^2}}{(a^2c^2 + c^2w^2 + a^2z^2)^{3/2}(w^2 + z^2 + a^2 + c^2 + 2\sqrt{a^2c^2 + c^2w^2 + a^2z^2})^{3/2}} \quad (4.10)$$

FIG. 5.—Axis ratio ξ of the surfaces of constant density as function of z

In the limit $c = a$ we have $v = a^2$, and the spheroidal coordinates reduce to spherical coordinates with $\lambda = r^2 + a^2$. In this case the potential reduces to

$$\psi(\lambda) = G(\lambda) = \frac{GM}{a + \sqrt{\lambda}} = \frac{GM}{a + \sqrt{r^2 + a^2}}. \quad (4.11)$$

The corresponding density distribution is

$$\rho(r) = \frac{Ma}{4\pi} \frac{a + 2\sqrt{r^2 + a^2}}{(r^2 + a^2)^{3/2}(a + \sqrt{r^2 + a^2})^2}. \quad (4.12)$$

Thus, in the spherical limit the Kuzmin-Kutuzov model is identical to Hénon's (1959) isochrone.

b) Dimensions

For the calculation of distribution functions it is convenient to work with dimensionless quantities. We choose as independent dimensional scale factors the length scale $a + c$, the total mass M , and the value of the potential at the center, which is equal to $G(a^2)$, and is given by

$$\psi_s = \frac{GM}{a + c}. \quad (4.13)$$

This determines our units of mass, length, and time. For convenience, Table 1 lists all relevant physical quantities with their range of definition and their dimensional scale factors. *In what follows, all symbols should be interpreted as referring to dimensionless quantities.* In particular,

$$\psi(0, 0) = 1, \quad GM = 1, \quad a + c = 1, \quad (4.14)$$

so that $0 \leq a \leq 1$ and $0 \leq c \leq 1$.

The definition (4.1) of $G(\tau)$ is not invariant under addition of a constant in the definition of λ and v , which means that the definition (4.1), despite its appearance, involves two constants. However, due to the normalization $a + c = 1$ expression (4.1) describes a one-parameter family of axisymmetric Stäckel potentials.

c) Two Integral Model: $F = F(E, I_2)$

Kuzmin and Kutuzov (1962) showed that the model defined in § IVa has the remarkable property that ρ can be expressed explicitly in terms of ϖ and ψ . As we have seen in § IIIb, the explicit expression $\rho(\varpi, \psi)$ is required for the successful construction by analytic means of the even part $F(E, I_2)$ of the distribution function F that is consistent with ρ . Kuzmin and Kutuzov (1962) state that they have obtained $F(E, I_2)$ by means of Fricke's (1952) method. However, they do not give F explicitly, but instead show contours of F in the (E, L_z) -plane, and furthermore give a plot of the velocity distribution. We now apply the more powerful inversion methods mentioned in § IIIb, and derive a convergent form of $F(E, I_2)$.

TABLE 1
DIMENSIONS

Quantity	Symbol	Unit	Range
Coordinate	ϖ, z	$a + c$	$[0, +\infty[$
	x, y, z, x', y'	$a + c$	$] -\infty, +\infty[$
	λ	$a + c$	$[\max(a^2, c^2), +\infty[$
	v	$a + c$	$[\min(a^2, c^2), \max(a^2, c^2)]$
Velocity	v_ϖ, v_ϕ, v_z	$\sqrt{\psi_s}$	$[-1, +1]$
	v_λ, v_v, v_p	$\sqrt{\psi_s}$	$[-1, +1]$
Velocity dispersion	$\sigma_\varpi, \sigma_\phi, \sigma_z$	$\sqrt{\psi_s}$	$[0, 1]$
	$\sigma_\lambda, \sigma_v, \sigma_p$	$\sqrt{\psi_s}$	$[0, 1]$
Potential	ψ	ψ_s	$[0, 1]$
Mass density	ρ	$M/(a + c)^3$	$[0, +\infty[$
Surface density	Σ	$M/(a + c)^2$	$[0, +\infty[$
Binding energy	E	ψ_s	$[0, 1]$
Angular momentum	L_z	$(a + c)\sqrt{\psi_s}$	$[0, +\infty[$
Third integral	I_3	$(a + c)^2\psi_s$	$[\min(a - c, 0), +\infty[$

For the specific form (4.2) of the potential ψ the following two relations hold:

$$\sqrt{\lambda} + \sqrt{v} = \frac{1}{\psi}, \quad \sqrt{\lambda v} = \frac{a}{\psi} (\sqrt{1 - A\varpi^2\psi^2} - a\psi), \tag{4.15}$$

where

$$A = \frac{a^2 - c^2}{a^2}. \tag{4.16}$$

Substitution in equation (4.3) for the density distribution produces

$$\rho = \rho(\varpi, \psi) = \frac{c^2}{4\pi a} \psi^4 \frac{(2 - A\varpi^2\psi^2 - a\psi\sqrt{1 - A\varpi^2\psi^2})}{(\sqrt{1 - A\varpi^2\psi^2} - a\psi)^3}. \tag{4.17}$$

This is the expression obtained by Kuzmin and Kutuzov (1962).

Introduce an auxiliary quantity X by

$$X = \frac{a\psi}{\sqrt{1 - A\varpi^2\psi^2}}, \tag{4.18}$$

and write equation (4.17) as

$$\rho(\varpi, \psi) = \frac{c^2}{4\pi a} \psi^4 \left[\frac{(1 - A\varpi^2\psi^2)^{-3/2}}{(1 - X)^3} + \frac{(1 - A\varpi^2\psi^2)^{-1/2}}{(1 - X)^2} \right]. \tag{4.19}$$

It is easily seen, by writing X as

$$X = \frac{a^2}{a^2 + \sqrt{\lambda v}} = \frac{a^2}{a^2 + \sqrt{a^2c^2 + c^2\varpi^2 + a^2z^2}}, \tag{4.20}$$

that $0 \leq X \leq a$ for all values of ϖ and z . The case $a = 1$, and thus $c = 0$, corresponds to Kuzmin's (1953) disk and is excluded here, since it is not possible to construct a self-consistent disk with a nonsingular distribution function in three-dimensional velocity space. Consequently, we may expand equation (4.19) as follows

$$\rho(\varpi, \psi) = \frac{c^2}{8\pi a} \sum_{k=0}^{\infty} (k + 1)a^k\psi^{k+4} [2(1 - A\varpi^2\psi^2)^{-(k+1)/2} + (k + 2)(1 - A\varpi^2\psi^2)^{-(k+3)/2}]. \tag{4.21}$$

D86 (eq. [2.5.54]) gives the distribution function $F(E, L_z^2)$ that is consistent with an axisymmetric density $\rho(\varpi, \psi) = \psi^s(1 - \varpi^2\psi^2)^t$, with s and t arbitrary (see also Appendix C). By repeated application of this result we find for the density given in equation (4.21) the following (even part of the) distribution function:

$$F(E, L_z^2) = \frac{1}{(2\pi)^{5/2}} \frac{c^2}{4a} E^{5/2} \sum_{k=0}^{\infty} (k + 1) \frac{\Gamma(k + 5)}{\Gamma(k + 7/2)} (aE)^k \times \left[2 {}_3F_2\left(\frac{k}{2} + \frac{5}{2}, \frac{k}{2} + 3, \frac{k}{2} + \frac{1}{2}; k + \frac{7}{2}, \frac{1}{2}; 2AEL_z^2\right) + (k + 2) {}_3F_2\left(\frac{k}{2} + \frac{5}{2}, \frac{k}{2} + 3, \frac{k}{2} + \frac{3}{2}; k + \frac{7}{2}, \frac{1}{2}; 2AEL_z^2\right) \right], \tag{4.22}$$

where ${}_3F_2$ is a generalized hypergeometric function, defined as

$${}_3F_2(a, b, c; d, e; z) = \frac{\Gamma(d)\Gamma(e)}{\Gamma(a)\Gamma(b)\Gamma(c)} \sum_{n=0}^{\infty} \frac{\Gamma(a+n)\Gamma(b+n)\Gamma(c+n)}{\Gamma(d+n)\Gamma(e+n)} \frac{z^n}{n!}. \quad (4.23)$$

The series expansion (4.23) for ${}_3F_2$ has radius of convergence $|z| = 1$. It is not difficult to show that (D86, eq. [2.5.90])

$$0 \leq 2|A|EL_z^2 \leq |A|\varpi^2\psi^2 \leq \frac{|a^2 - c^2|}{a^2}. \quad (4.24)$$

As a result, as long as $a_c = 1/[1 + \sqrt{2}] < a < 1$, all terms in the series (4.22) for F are well-defined. When $a < a_c$, however, we need the analytic continuation of equation (4.23) for $-\infty < z < -1$, since then the generalized hypergeometric functions do not converge for all values of E and L_z^2 . This analytic continuation is obtained by observing that all the generalized hypergeometric functions in equation (4.22) are of the form

$${}_3F_2\left(\frac{k}{2} + \frac{5}{2}, \frac{k}{2} + 3, \frac{k}{2} + \frac{p}{2}; k + \frac{7}{2}, \frac{1}{2}; z\right), \quad p = 1, 3, \quad (4.25)$$

for which an integral representation is known (Gradshteyn and Ryzhik, eq. [7.512.12]):

$$\frac{\Gamma(k+7/2)}{\Gamma[(k+p)/2]\Gamma[(k+7-p)/2]} \int_0^1 u^{(k+p)/2-1} (1-u)^{(k+5-p)/2} {}_2F_1\left(\frac{k+5}{2}, \frac{k+6}{2}; \frac{1}{2}; zu\right) du. \quad (4.26)$$

The integrand now contains an ordinary hypergeometric function, which happens to be expressible in terms of simple algebraic functions (Erdelyi 1953, eq. [2.8 (5)]):

$${}_2F_1\left(\frac{k+5}{2}, \frac{k+6}{2}; \frac{1}{2}; zu\right) = \frac{1}{2} [(1 - \sqrt{zu})^{-(k+5)} + (1 + \sqrt{zu})^{-(k+5)}]. \quad (4.27)$$

If we substitute equations (4.25), (4.26), and (4.27) in equation (4.22), we can actually carry out the summations, and obtain

$$F(E, L_z^2) = \frac{1}{2^{3/2}\pi^3} \frac{c^2}{a} E^{5/2} \left\{ \sum_{\epsilon=-1,1} \int_0^1 \frac{(1-t^2)}{(1+2aEt\sqrt{1-t^2} + \epsilon t\sqrt{z})^5} [(3+4x_\epsilon - x_\epsilon^2)(1-x_\epsilon^2)(1-t^2) + 12t^2] dt \right\}, \quad (4.28a)$$

with

$$x_\epsilon = \frac{2aEt\sqrt{1-t^2}}{1 + \epsilon t\sqrt{z}}, \quad z = 2AEL_z^2. \quad (4.28b)$$

This form for $F(E, L_z^2)$ is well-defined for all values of E and L_z^2 , subject to the constraint equation (4.24), for all allowed values of a and c . The remaining integration in the variable t can be performed easily by numerical means.

We have numerically evaluated $F(E, L_z^2)$ given in equations (4.22) and (4.28) for a range of values of a and c . It turns out that the two-integral distribution function is nowhere negative for $c < a$, so that all oblate models are physical. For prolate models, however, we find that $F(E, L_z^2)$ becomes negative for some values of E and L_z^2 for $c/a \gtrsim 1.35$. This is still below the critical value above which the series (4.22), and the expressions for the velocity moments given in Appendix C, breaks down. It follows that highly elongated prolate Kuzmin-Kutuzov models with a two-integral distribution function do not exist. As an example, we show in Figure 6 the distribution function in the (E, L_z^2) -plane, for the cases $c/a = 0.5$ and $c/a = 1.25$. Upon comparison with Figure 2, it is evident that for the chosen axis ratio, most of the orbits in the prolate model are outer long axis tubes.

The velocity dispersions σ_ϖ , σ_ϕ , and σ_z can be calculated with the general formulae (3.33) and (3.32). For the density of the elementary model, the integrals (3.32) can be done in closed form. After introduction of the variable Y , defined as

$$Y = -\frac{A\varpi^2}{a^2}, \quad (4.29)$$

we obtain after somewhat lengthy calculations, aided by the symbolic manipulation program MACSYMA,

$$\begin{aligned} \rho\sigma_\varpi^2 = & \frac{c^2}{4\pi a^6} \left[h_\varpi(\sqrt{Y}) + h_\varpi(-\sqrt{Y}) + \frac{1}{(1-Y)^3} \left\{ -2 \frac{(1+2Y)}{1-Y} \ln(1-X) + \frac{X}{8Y(1-YX^2)^2} \right. \right. \\ & + \frac{X}{8(1-YX^2)^2(1-X)^2} [(4Y^3 + 20Y^2)X^5 + (-8Y^3 - 17Y^2 + 1)X^4 + (-6Y^2 - 44Y + 2)X^3 \\ & \left. \left. + (15Y^2 + 39Y - 7)X^2 + (2Y + 24)X - 9Y - 16 \right\} \right], \quad (4.30) \end{aligned}$$

AXISYMMETRIC THREE-INTEGRAL MODELS

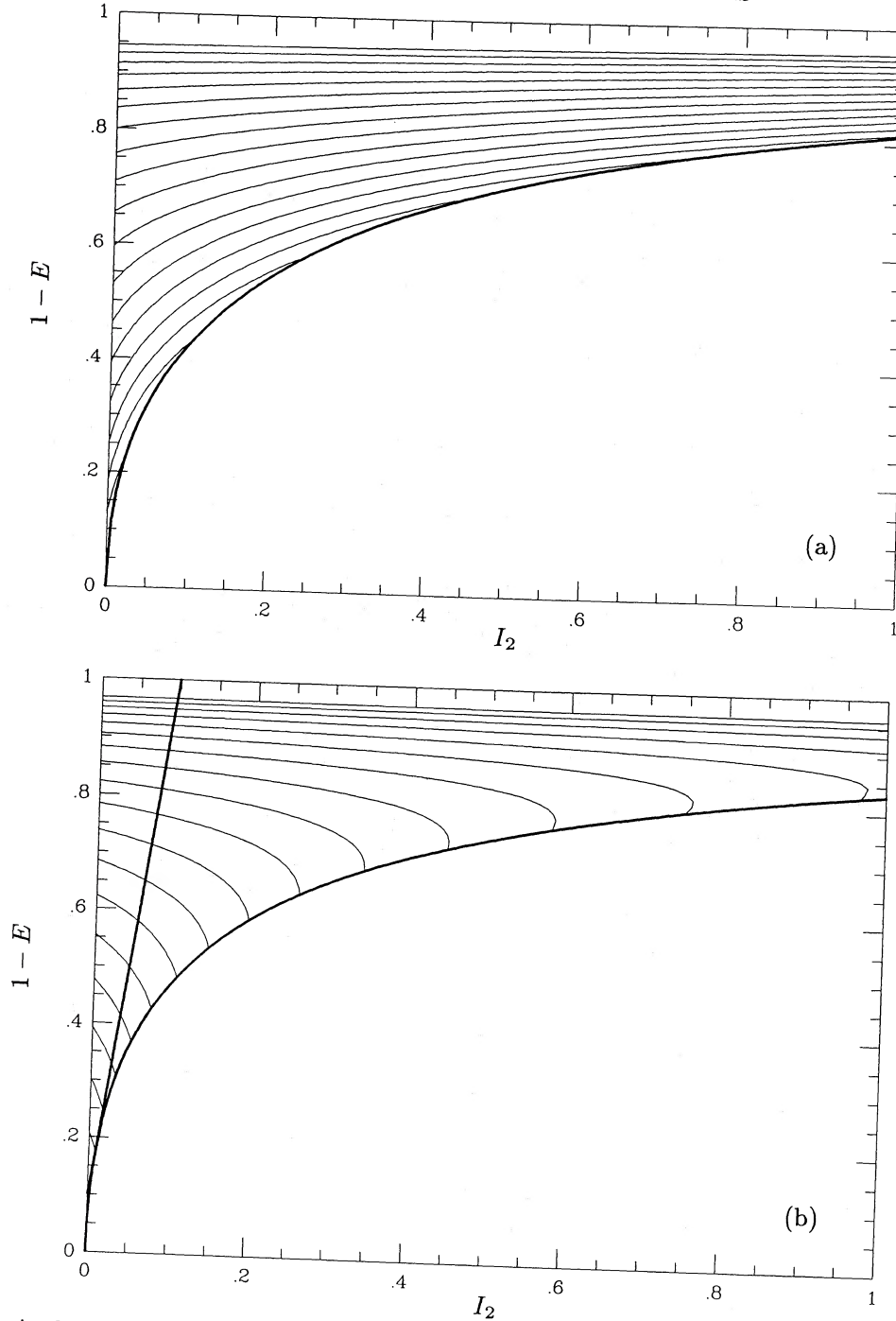


FIG. 6.—Distribution function $F(E, I_2)$ for (a) $c/a = 0.5$ and (b) $c/a = 1.25$. Contours are logarithmically spaced. Heavy curves correspond to the boundaries shown in more detail in Figs. 1 and 2.

and

$$\rho(\sigma_\phi^2 + \langle v_\phi \rangle^2) = \frac{c^2}{4\pi a^6} \left[h_\phi(\sqrt{Y}) + h_\phi(-\sqrt{Y}) + \frac{1}{(1-Y)^4} \left\{ -2 \frac{(1+13Y+10Y^2)}{1-Y} \ln(1-X) - \frac{X}{4Y(1-YX^2)^2} \right. \right. \\ \left. \left. - \frac{X}{4(1-YX^2)^2(1-X)^3} [2Y(2Y^4 - 5Y^3 + 48Y^2 + Y + 2)X^6 + (-14Y^4 - 170Y^3 + Y^2 - 12Y + 3)X^5 \right. \right. \\ \left. \left. + (8Y^4 + 98Y^3 - 191Y^2 - 4Y - 7)X^4 + (30Y^3 + 329Y^2 + 19Y + 7)X^3 \right. \right. \\ \left. \left. + (-30Y^3 - 161Y^2 + 91Y + 1)X^2 + (-14Y^2 - 167Y - 8)X + 18Y^2 + 73Y + 4 \right\} \right], \quad (4.31)$$

where $X = X(\varpi, z)$ is given in equation (4.20), and we have defined the auxiliary functions

$$h_{\varpi}(x) = \frac{(1 - 4x + 9x^2)}{16x^3(1-x)^4} \ln(1 - xX), \quad h_{\phi}(x) = \frac{(1 + 5x + 10x^2 + 18x^3)}{8x^3(1+x)^5} \ln(1 + xX). \quad (4.32)$$

For oblate models, $A > 0$, so that $Y < 0$. The functions h are then complex, but since we add complex conjugate terms, the result is real. This is not a problem for the computations. However, if we want a real form we find

$$\begin{aligned} h_{\varpi}(ix') + h_{\varpi}(-ix') &= \frac{1}{(1+x'^2)^4} \left[(1 - 2x'^2) \ln(1 + x'^2 X^2) + \frac{1 + x'^2 + 39x'^4 - 9x'^6}{8x'^3} \arctan x'X \right], \\ h_{\phi}(ix') + h_{\phi}(-ix') &= \frac{1}{(1+x'^2)^5} \left[(1 - 13x'^2 + 10x'^4) \ln(1 + x'^2 X^2) + \frac{-1 - 5x'^2 + 35x'^4 - 135x'^6 - 18x'^8}{4x'^3} \arctan x'X \right]. \end{aligned} \quad (4.33)$$

For prolate models the quantity Y is positive. In case $Y = 1$ both the numerator and the denominator in expressions (4.30) and (4.31) become zero, and we find

$$\begin{aligned} \rho \sigma_{\varpi}^2 &= \frac{c^2}{4\pi a^6} \left\{ -\frac{7}{128} \log \frac{1+X}{1-X} + \frac{[-16X^6 + 53X^5 + 70X^4 - 14X^3 - 42X^2 + 21X]}{192(X-1)^4(X+1)^2} \right\}, \\ \rho(\sigma_{\phi}^2 + \langle v_{\phi} \rangle^2) &= \frac{c^2}{4\pi a^6} \left\{ \frac{17}{128} \log \frac{1+X}{1-X} + \frac{[1072X^7 + 369X^6 - 1523X^5 + 1020X^4 + 340X^3 - 765X^2 + 255X]}{960(X-1)^5(X+1)^2} \right\}. \end{aligned} \quad (4.34)$$

The factors $(1 - YX^2)$ and $(1 - X)$ that also occur in the denominators of expressions (4.30) and (4.31) do not vanish.

We will not attempt to evaluate the double integral (3.33) for the calculation of $\langle v_{\phi}^{\pm} \rangle$ directly. We rather rely on equation (4.21) and the results of Appendix C. This yields an infinite sum of generalized hypergeometric functions which converges for all values of $a > a_c$, so that it covers all physical cases, and can be evaluated numerically without trouble. An example of the behavior of the mean stellar streaming motions will be given in § V.

d) Three Integral Models

The construction of three-integral models that are consistent with the Kuzmin-Kutuzov mass model proceeds essentially as outlined in § IIIb. We write $F(E, I_2, I_3)$ as the sum of $F_1(E, I_2)$ and $F_2(E, I_2, I_3)$, where F_2 is a finite sum of the form (3.13). The density of the model can be similarly decomposed as $\rho = \rho_1 + \rho_2$ (see eqs. [3.20] and [3.21]).

First we consider the case where F_2 consists of only one component $a_{lmn} E^l I_2^m (I_2 + I_3)^n$. Then $\rho_2 = a_{lmn} \rho_{lmn}$, with ρ_{lmn} given in equation (3.15). The next task is to find the two-integral distribution function F_1 that must be added to F_2 in order to make the model self-consistent, in accordance with equation (3.21). Therefore, we need to write equation (3.15) as a function of ϖ and ψ , as prescribed by equation (3.22). This is possible due to the particularly simple form of the potential. We find, after some rearrangement of terms,

$$\begin{aligned} \rho_2(\varpi, \psi) &= a_{lmn} 2^{3/2-n} \sqrt{\pi} n! \Gamma(l+1) \varpi^{2m} \psi^{l+m-n+3/2} \sum_{k=0}^n \frac{1}{\Gamma(3/2+m+k)} \sum_{i=0}^{k/2} \frac{\Gamma(i+1/2)\Gamma(1/2+m+k-2i)}{i!(k-2i)!} \\ &\times (1 - 4a\psi \sqrt{1 - A\varpi^2\psi^2} + 4a^2\psi^2)^i (1 - 2a\psi \sqrt{1 - A\varpi^2\psi^2})^{k-2i} \sum_{j=0}^{n-k} \frac{\Gamma(m+n+3/2-j)}{\Gamma(l+m+n+5/2-j) j! (n-k-j)!} \frac{2^j \psi^j}{j!} \\ &\times [(c^2 - a^2)\psi - c + a\sqrt{1 - A\varpi^2\psi^2}]^j [1 - 2a\psi \sqrt{1 - A\varpi^2\psi^2} + 2(a^2 - c^2)\psi^2]^{n-j-k}. \end{aligned} \quad (4.35)$$

It must be stressed that the ability to write ρ_2 explicitly as a function of ϖ and ψ depends critically on the simple form of the potential. Other Stäckel potentials may not allow such an explicit expression.

Upon expansion of equation (4.35) we find

$$\begin{aligned} \rho_2(\varpi, \psi) &= 2^{3/2-n} \sqrt{\pi} a_{lmn} n! \Gamma(l+1) \varpi^{2m} \psi^{l+m-n+3/2} \sum_{k=0}^n \frac{1}{\Gamma(3/2+m+k)} \sum_{i=0}^{k/2} \frac{\Gamma(i+1/2)\Gamma(1/2+m+k-2i)}{i!(k-2i)!} \\ &\times \sum_{i_1=0}^i \binom{i}{i_1} (2a)^{2i_1} \sum_{i_2=0}^{i-i_1} \binom{i-i_1}{i_2} (-4a)^{i_2} \sum_{i_3=0}^{k-2i} \binom{k-2i}{i_3} (-2a)^{i_3} \psi^{2i_1+i_2+i_3} (1 - A\varpi^2\psi^2)^{(i_2+i_3)/2} \\ &\times \sum_{j=0}^{n-k} \frac{\Gamma(m+n+3/2-j)}{\Gamma(l+m+n+5/2-j) j! (n-k-j)!} \sum_{j_1=0}^j \binom{j}{j_1} \left(\frac{a-c}{c}\right)^{j_1} \sum_{j_2=0}^{j-j_1} \binom{j-j_1}{j_2} (-c)^{-j_2} a^{j_2} \\ &\times \sum_{j_3=0}^{n-j-k} \binom{n-j-k}{j_3} [2(a-c)]^{j_3} \sum_{j_4=0}^{n-j-k-j_3} \binom{n-j-k-j_3}{j_4} (-2a)^{j_4} \psi^{j+j_1+2j_3+j_4} (1 - A\varpi^2\psi^2)^{(j_2+j_4)/2}. \end{aligned} \quad (4.36)$$

It is apparent that the above expression can be written as a double but finite sum of terms of the form

$$\rho_2(\varpi, \psi) = \sum_{\rho=l+m-n+3/2}^{l+m+n+3/2} \sum_{\sigma=0}^n a_{lmn} B_{\rho, \sigma} \varpi^{2m} \psi^{\rho} (1 - A\varpi^2\psi^2)^{\sigma/2}, \quad (4.37)$$

where the $B_{\rho, \sigma}$ are constants. We will not make the series (4.37) mathematically explicit, but leave this mechanical operation to a computer.

The two-integral distribution function that corresponds to a density of the form $\varpi^{2m}\psi^\rho(1 - A\varpi^2\psi^2)^{\sigma/2}$ can be derived by means of the inversion method described in D86. The resulting expression, and all the velocity moments, are given in Appendix C. Summation of the individual expressions gives the two-integral distribution function $a_{lmn} F_{lmn}(E, L_z^2)$ that is consistent with ρ_2 . As a result, we may write the exact distribution function $F(E, I_2, I_3)$ of our model as

$$F(E, L_2, I_3) = F(E, L_z^2) + a_{lmn}[E^l I_2^m (I_2 + I_3)^n - F_{lmn}(E, L_z^2)], \quad (4.38)$$

where $F(E, L_z^2)$ is the two-integral distribution function that is consistent with ρ , calculated in § IVc, and

$$F_{lmn}(E, L_z^2) = \frac{1}{2\sqrt{2\pi}} \sum_{\rho, \sigma} B_{\rho, \sigma} \frac{\Gamma(\rho + 1)}{\Gamma(\rho - m - 1/2)\Gamma(m + 1/2)} E^{\rho - m - 3/2} I_2^m {}_3F_2\left(\frac{1 + \rho}{2}, 1 + \frac{\rho}{2}, -\frac{\sigma}{2}; \rho - m - \frac{1}{2}, \frac{1}{2} + m; 2AEL_z^2\right). \quad (4.39)$$

Similar expressions may be given for all the velocity moments. The convergence of the generalized hypergeometric functions is discussed in Appendix C. It is evident that the above process can be repeated for a sum of components $a_{lmn} E^l I_2^m (I_2 + I_3)^n$.

e) Hénon's Isochrone

In the spherical limit, $c = a = \frac{1}{2}$, the two-integral distribution function $F(E, L_z^2)$ obtained in § IVc reduces to an isotropic distribution function $F = F(E)$, with

$$F(E) = \frac{E^{5/2}}{8(2\pi)^{5/2}} \sum_{k=0}^{\infty} (k+1)(k+4) \frac{\Gamma(k+5)}{\Gamma(k+7/2)} \left(\frac{E}{2}\right)^k. \quad (4.40)$$

This is equivalent to the result that can be derived by straightforward application of Eddington's (1915b) inversion formula, which can be written as (Hénon 1960; Dejonghe 1984; Binney and Petrou 1985)

$$F(E) = \frac{1}{4\sqrt{2\pi^3}} \left[\frac{(4E^4 - 30E^3 + 80E^2 - 33E + 27)}{(2-E)^4} \sqrt{E} + \frac{3(4E^2 + 14E - 9)}{(2-E)^{9/2}} \arccos(1-E) \right]. \quad (4.41)$$

The velocity dispersions given in equations (4.30) and (4.31) reduce to the same expression:

$$\rho \langle v_r^2 \rangle = \rho \langle v_\phi^2 \rangle = \frac{1}{\pi} \left[\frac{1}{6} \psi^3 + \frac{1}{2} \psi^2 + 10 + 8 \frac{3\psi - 5}{(2-\psi)^2} + 8 \log \frac{2}{2-\psi} \right], \quad (4.42)$$

where $\psi = \psi(r)$ is given in equation (4.11).

The limiting form of the density that corresponds to the three-integral component in equation (4.38) was given in equation (3.35). The function $F_{lmn}(E, L_z^2)$ defined in equation (4.39) reduces to

$$F_{lmn}(E, L_z^2) = \frac{\Gamma(l+1)\Gamma(l+m-n+5/2)\Gamma(m+n+1)}{\Gamma(l-n+1)\Gamma(l+m+n+5/2)\Gamma(m+1)} E^{l-n} I_2^m {}_2F_1\left(l+m-n+\frac{5}{2}, -n; l-n+1; E\right). \quad (4.43)$$

Since n is an integer, the hypergeometric function is a finite sum. This was to be expected, since expression (4.43) is the limiting form of the finite sum (4.39). Thus, our construction yields genuine three-integral spherical isochrone models.

f) Examples

We have now concluded the mathematical presentation of the three-integral models. We close § III with a brief discussion of some individual components.

Figure 7 shows the density distribution in the meridional plane of four components ρ_{lmn} , defined in equation (3.15), for the potential of the Kuzmin-Kutuzov model with $c/a = 0.5$. The density distribution in terms of ϖ and ψ is given in equation (4.36). Components ρ_{100} are defined as the density corresponding to a distribution function that depends on E only, so that the surfaces of constant density are equipotential surfaces. These are less flattened than the surfaces of constant density for the whole model. The case ρ_{500} is shown in Figure 7a. Figure 7b presents ρ_{520} , which has a density distribution that is toroidal, with the highest density along a circle in the equatorial plane, and zero density along the symmetry axis. This shape is caused by the dependence on I_2 , and is characteristic for all components with $m \neq 0$. A third example (Fig. 7c) is ρ_{804} , which is more elongated along the symmetry axis, and has a minimum in the center. The final example shows a linear combination of two components, $\rho_{811} + 0.001\rho_{600}$, which gives rise to a boxlike density distribution. Clearly, there is a wide variety of individual three-integral components.

In order to calculate the dispersions for a component, the relevant moments have been divided by the density ρ of the complete model, given in equation (4.3). The resulting quantity is proportional to the partial pressure contributed by the component in the potential of the Kuzmin-Kutuzov model. The size of the velocity ellipsoid is proportional to the square root of the partial pressure. In Figure 8, we show the velocity ellipsoids for the component ρ_{804} for the oblate model with $c/a = 0.5$ and the prolate model with $c/a = 1.25$, superposed on the contours of constant density in the meridional plane. The velocity ellipsoids are defined at each position as the ellipsoids in velocity space (v_λ, v_ϕ, v_v) that have semiaxes equal to $\sigma_\lambda, \sigma_\phi$, and σ_v , and are aligned along the coordinate lines (see § IIIc). Following Petrou (1983a, b), we indicate the shape of the velocity ellipsoids by their sections with the (v_λ, v_v) -plane (*full ellipse*) and the (v_ϕ, v_v) -plane (*dotted ellipse*), respectively. The outer dotted ellipse is for the case of no net streaming, and the inner dotted ellipse is for the case where all stars have the same sense of rotation around the z -axis, so that σ_ϕ is smaller. It is evident

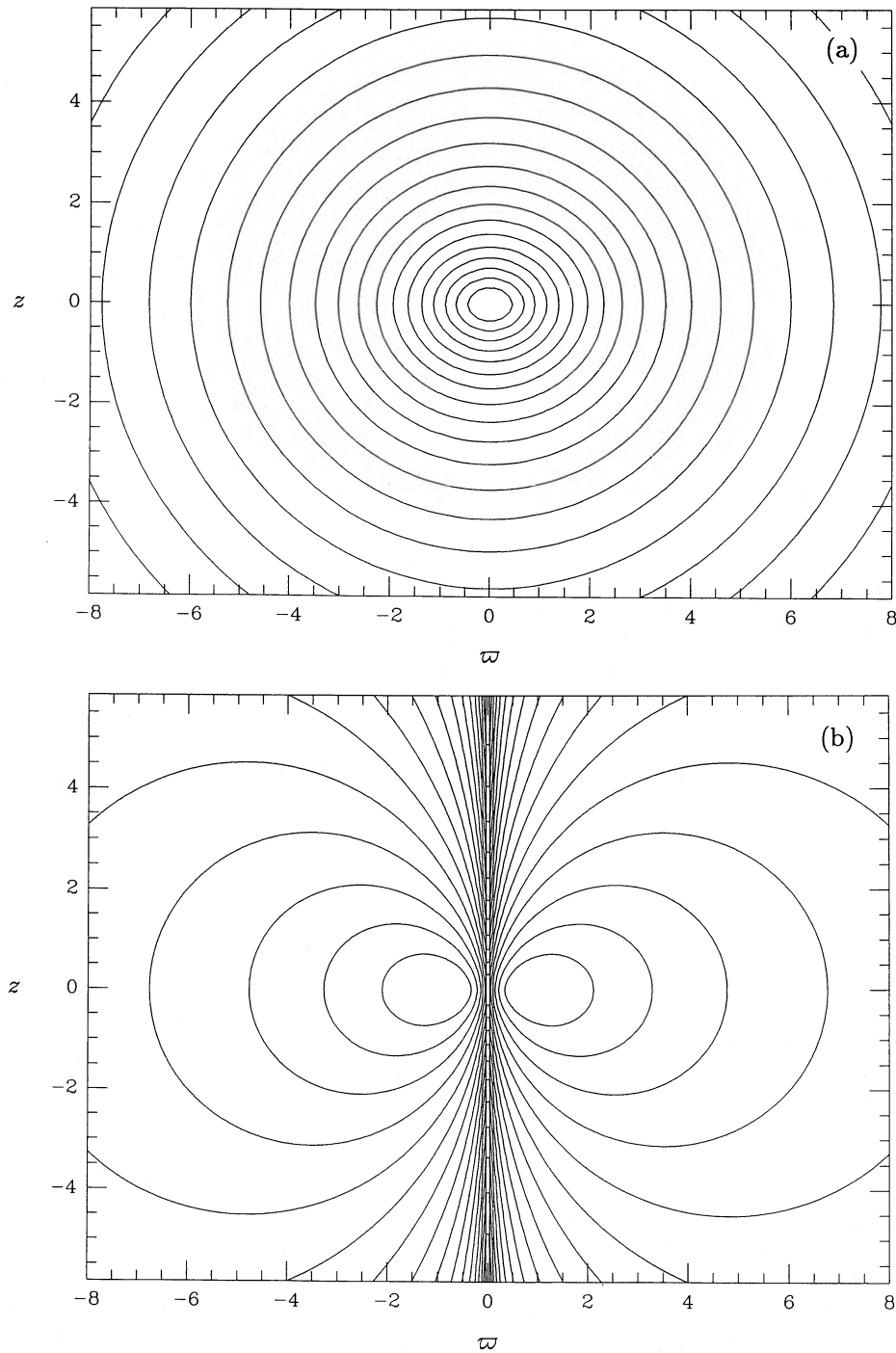


FIG. 7.—Contours of constant density in the meridional plane for components ρ_{lmn} defined in eq. (3.15) in the potential of the Kuzmin-Kutuzov model. (a) ρ_{500} . (b) ρ_{520} . (c) ρ_{804} . (d) $\rho_{811} + 0.001\rho_{600}$.

that the velocity ellipsoids for this particular component are most elongated in the v -direction. For the case shown, the inner dotted ellipse is nearly indistinguishable from the full ellipse, so that the velocity ellipsoids are nearly spheroidal.

The filled squares in Figure 8 indicate the foci of the spheroidal coordinates. According to equation (D9), here $\sigma_\lambda = \sigma_\phi = \sigma_v$ for the case of no net streaming. This is suggested by the shape of the velocity ellipsoids in the points neighboring the foci as shown in Figure 8a. In the presence of streaming only σ_λ and σ_v are equal at the foci.

Finally, in Figures 9 and 10, we present the velocity ellipsoids for self-consistent distribution functions for the oblate and prolate Kuzmin-Kutuzov models with the same axis ratios as used in Figure 8. The cases with a two-integral distribution function $F(E, L_z^2)$ have been calculated with the help of equations (4.30) and (4.31), and are illustrated in Figures 9a and 10a. The velocity ellipsoids now are spheroids, since $\sigma_\lambda = \sigma_v$ everywhere. In Figures 9b and 10b we give the velocity ellipsoids for a three-integral distribution

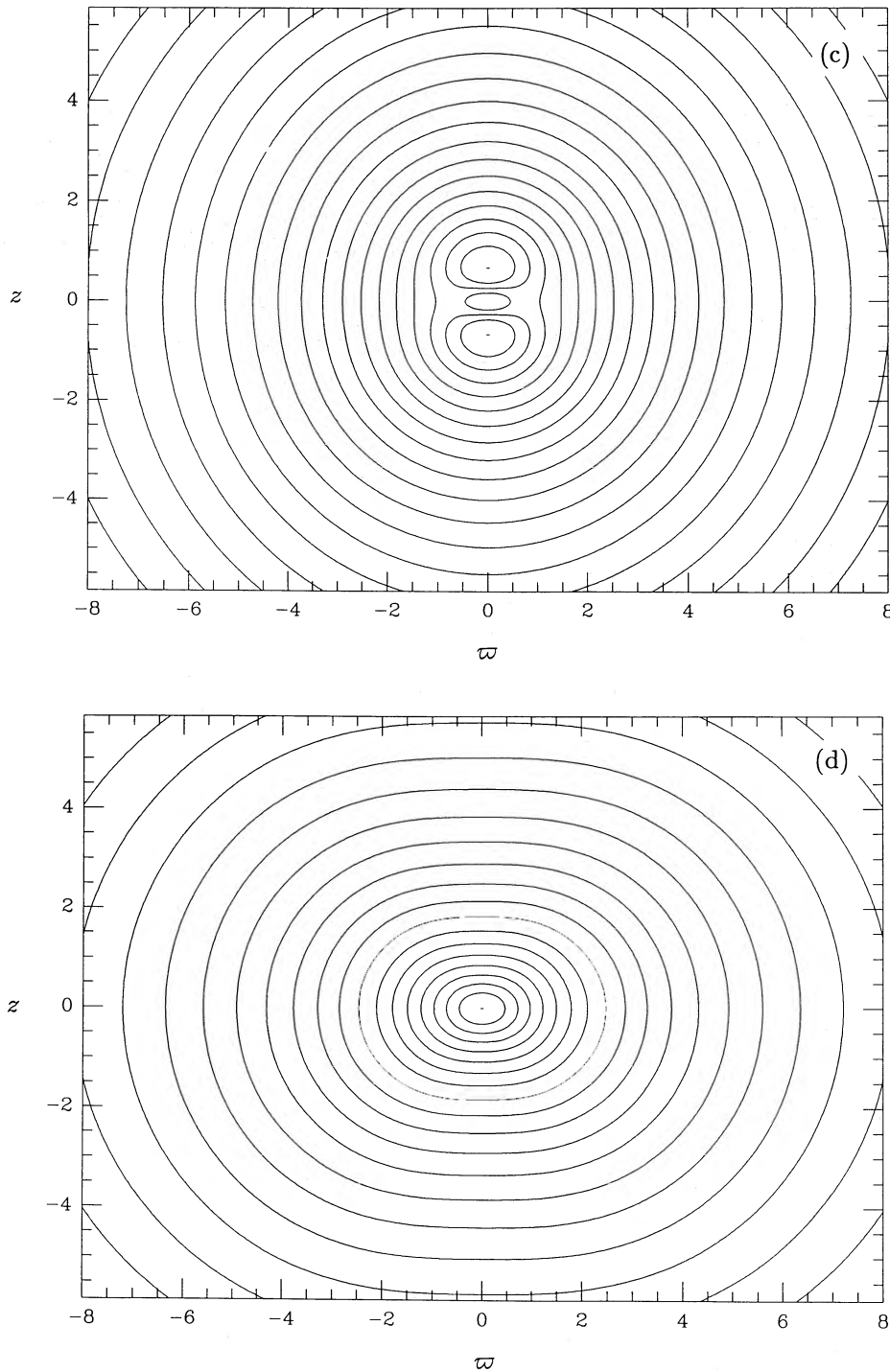


FIG. 7.—Continued

function of the form (4.38), with only one component ρ_{lmn} . As an example, we have taken the component ρ_{501} , and have chosen $a_{501} = -1.9$ in the oblate case, and $a_{501} = -5.0$ in the prolate case.

We have seen in § IVc that the prolate Kuzmin-Kutuzov models with distribution functions $F(E, L_z^2)$ are unphysical, i.e., have $F(E, L_z^2) < 0$ for some values of E and L_z^2 , for $c/a \gtrsim 1.35$. This does not mean that no self-consistent dynamical models with $F = F(E, L_z^2, I_3)$ exist for those axis ratios. We expect that they can be found by a judicious choice of components ρ_{lmn} .

V. OBSERVABLE PROPERTIES

As an example, we again consider the oblate model with $c/a = 0.5$ and the prolate model with $c/a = 1.25$, and calculate a number of observable properties.

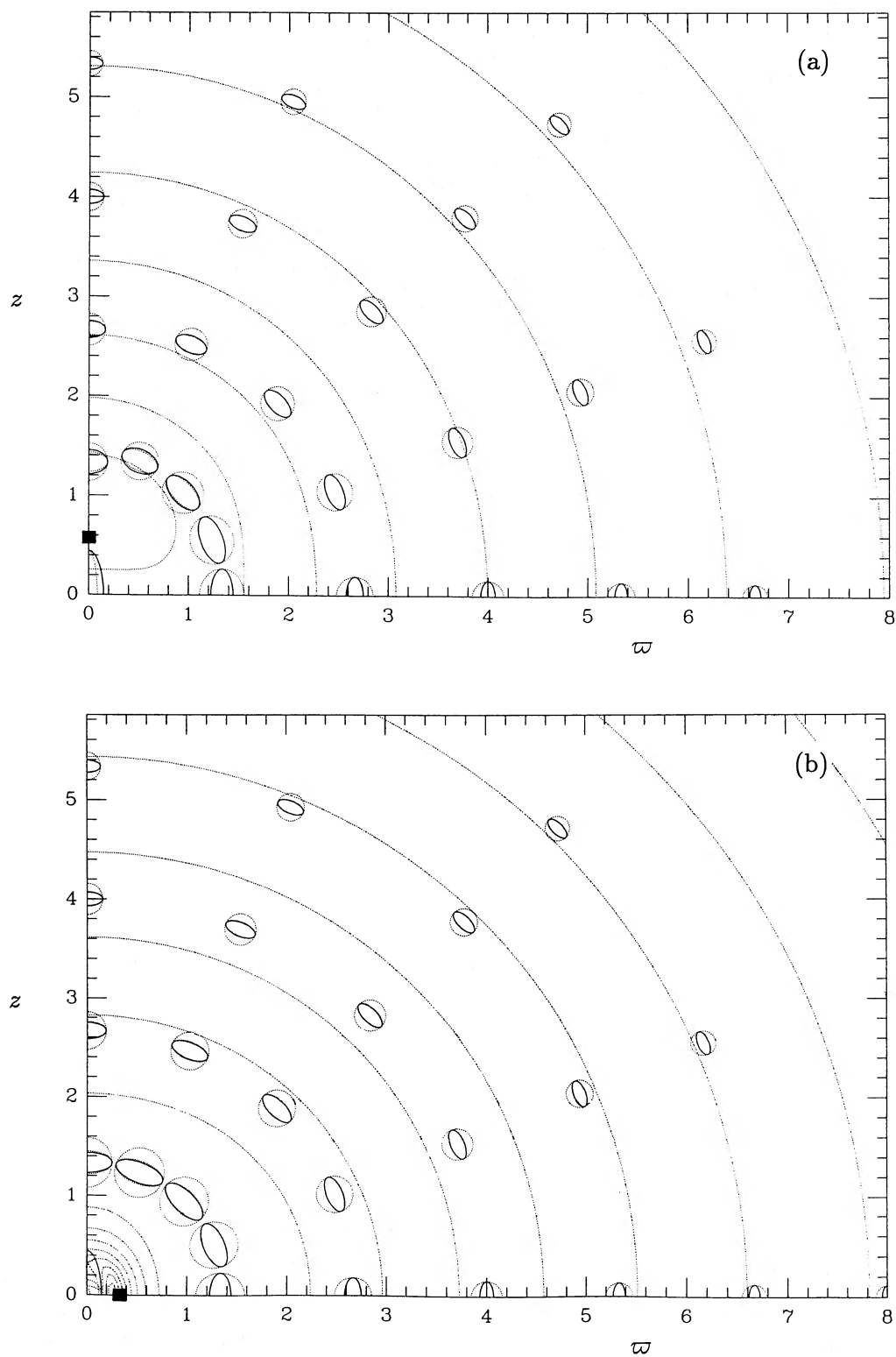


FIG. 8.—Velocity ellipsoids for the component ρ_{004} , superposed on the contours of constant density in the meridional plane. Full ellipse shows the section with the (v_λ, v_ν) -plane. Outer dotted ellipse is the section with the (v_ϕ, v_ν) -plane. Inner dotted ellipse is the same, but for the equivalent right-handed model. Further details are given in the text. (a) $c/a = 0.5$. (b) $c/a = 1.25$.

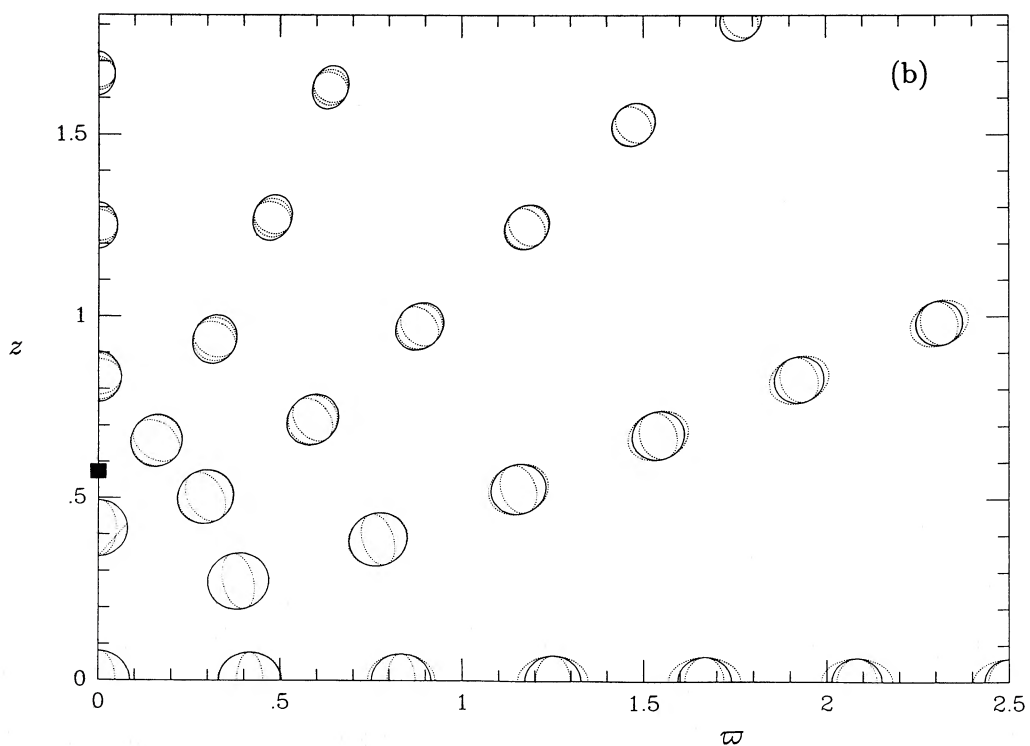
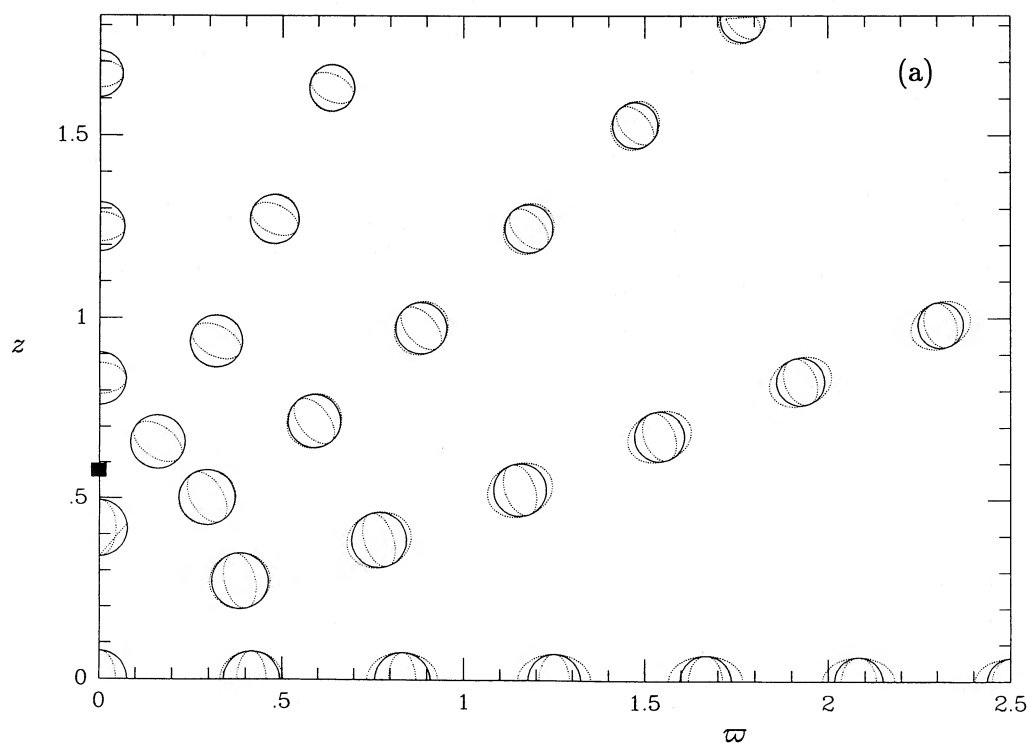


FIG. 9.—Velocity ellipsoids for oblate self-consistent Kuzmin-Kutuzov models with $c/a = 0.5$. (a) $F = F(E, L_z)$. (b) F is of the form (4.38) with $a_{501} = -1.9$.

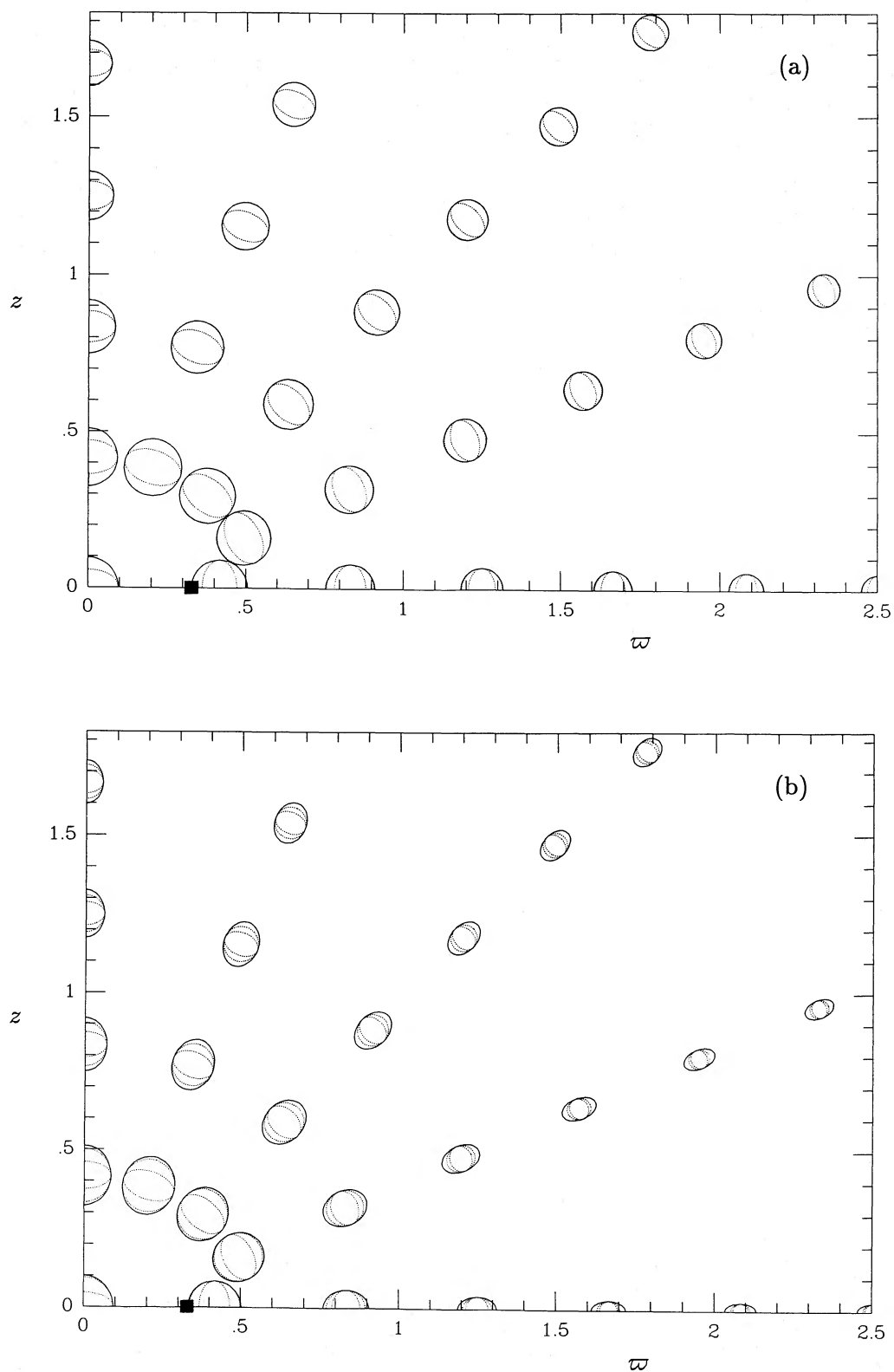


FIG. 10.—Velocity ellipsoids for prolate self-consistent Kuzmin-Kutuzov models with $c/a = 1.25$. (a) $F = F(E, L_z)$. (b) F is of the form (4.38) with $a_{5,01} = -5.0$.

a) *Projected Surface Density*

It is possible to calculate the projected surface density Σ of the Kuzmin-Kutuzov models for any direction of viewing by analytic means. This is not obvious from the expressions (4.3) or (4.10) for the density, but is due to a property of the models that was already discovered by Kuzmin (1956). He showed that the models are members of a much larger family of Stäckel models all of which can be considered as a weighted sum of perfect spheroids (Z85), with different axis ratios. As a result, Σ is the same weighted sum of the projected surface densities of the constituent spheroids. These are known, since the density in a perfect spheroid is stratified on similar, concentric, spheroids of a fixed axis ratio, and hence it projects to a surface density distribution that is stratified on similar, concentric, ellipses (Contopoulos 1956; Stark 1977). It turns out that for the Kuzmin-Kutuzov models the resulting integral for Σ can be evaluated explicitly. The derivation is straightforward, but somewhat lengthy, and is given in Appendix E. The resulting Σ can be expressed in terms of incomplete elliptic integrals of the first and second kind, and is given in equations (E22) and (E23). It is easily evaluated numerically.

In Figure 11 we show the projected surface density of the two models we consider, for viewing angles θ with respect to the z -axis equal to 45° and 90° . We denote the coordinates in the plane of projection by (x', y') . They are chosen such that the projected z -axis falls along the y' -axis (see also Appendix E). Figure 12 shows the axis ratio ξ_p of the isophotes—the contours of constant projected surface density—as function of the distance along the y' -axis. It is evident that the isophotes are roughly elliptic, and show a small ellipticity variation. This is in agreement with the fact that the surfaces of constant density are approximately spheroidal, with an axis ratio that varies slowly with radius.

 b) *Kinematics*

Now we turn to the projected velocity dispersions σ_p , and, for the case where all the stars orbit in a definite direction (see § IIIa), to the mean streaming velocity v_p . These have been calculated by numerical integration of the velocity moments given explicitly in § IV. The relevant equations can be found, e.g., in Fillmore (1986). We consider the distribution function $F(E, L_z^2)$ derived in § IVc, as well as a three-integral distribution function of the form (4.38), with one component, ρ_{lmn} . As in § IVf, we take the component ρ_{501} , with $a_{501} = -1.9$ for the oblate model and $a_{501} = -5.0$ for the prolate model. Our restriction to just one three-integral component is not fundamental, but results from our intent to discuss a simple example, rather than to give a complete, and lengthy, description of all the self-consistent three-integral Kuzmin-Kutuzov models. We can add more components easily, and so obtain a larger variety in properties. In a future paper we expect to combine many components in a more mechanical manner (see also § VI).

The velocity field for the two models is presented in Figure 13. Figure 14 shows the mean streaming velocity $\langle v_\phi^+ \rangle$ for a viewing angle $\theta = 90^\circ$ (edge-on), as measured along the apparent major axis. For comparison, we have also drawn the rotation curve, i.e., the circular velocity $v_c(x')$. It is evident that in the oblate case the addition of this three-integral component to the two-integral model has little influence on the velocity field. In our prolate case the two velocity fields differ substantially. Here the additional component causes a considerable depression in the mean stellar streaming.

We emphasize that the curves shown have been computed for the case where all stars orbit in the same direction. As already noted in § IIIc, many rotational states between this extreme case and the case of no rotation are possible. In particular rotation curves that rise over a substantial fraction of the model can be obtained (see also D86).

The velocity dispersion σ_ϕ depends on the value of the mean stellar streaming motion, $\langle v_\phi \rangle$ (see § IIIc). For models with $F = F(E, L_z^2)$ it is customary to determine $\langle v_\phi \rangle$ by the requirement that the velocity dispersions are isotropic, i.e., $\sigma_\omega = \sigma_z = \sigma_\phi$ (e.g., Nagai and Miyamoto 1976; Satoh 1980). In Figure 15 we show the projected velocity dispersion field for the isotropic oblate Kuzmin-Kutuzov model, for $\theta = 90^\circ$. Due to the fact that σ_ω is a slowly varying function, this isotropic velocity dispersion field is very regular.

Whereas for models with $F = F(E, L_z^2)$ there is some justification for considering the isotropic case, for three-integral models generally $\sigma_\omega \neq \sigma_z$, so that the assumption of isotropy is impossible. As in Figures 13 and 14, we therefore again consider the case of maximum streaming for our two distribution functions. The corresponding projected velocity dispersion fields are shown in Figures 16 and 17. Clearly, in the oblate case the resulting velocity dispersion fields differ considerably from the isotropic one shown in Figure 15, even for $F = F(E, I_2)$. A corollary of this result is that, if a galaxy is observed to have a velocity dispersion field that is not as regular as the one of Figure 15, then one cannot immediately conclude that the galaxy is not oblate, or requires a distribution function that depends on three integrals.

VI. DISCUSSION

 a) *Analytic Axisymmetric Dynamical Models*

In this paper we have investigated the self-consistent problem for axisymmetric dynamical models with a potential of Stäckel form and a phase-space distribution function F that depends on three integrals of motion. In particular, we have shown how the Fricke (1952) method for the construction of models with $F(E, I_2)$ can be generalized, and we have derived the explicit expressions for the density components $\rho_{lmn}(\omega, z)$ that correspond to distribution functions of the form $F_{lmn} = E^l I_2^m (p + qE + rI_2 + 2sI_3)^n$ (see eq. [3.15]). If we can expand a given density ρ as $\rho = \sum a_{lmn} \rho_{lmn}$, then the corresponding distribution function is given by $F = \sum a_{lmn} F_{lmn}$. In general, there are many such expansions, and hence many different distribution functions.

Construction of exact three-integral models via direct application of the generalized Fricke method is severely limited by the cumbersome form of the individual components ρ_{lmn} . For that reason we modified the method, and specified a three-integral distribution function of the form $\sum a_{lmn} F_{lmn}$ with a finite number of terms only, and subsequently subtracted the corresponding density $\rho_2(\omega, z) = \sum a_{lmn} \rho_{lmn}(\omega, z)$ from the model density. By means of a standard inversion technique we then calculated the two-integral distribution function $F(E, I_2)$ that corresponds to the remaining density. By application of this method to a family of axisymmetric Stäckel models studied previously by Kuzmin and Kutuzov (1962) we found explicit three-integral distribution functions.

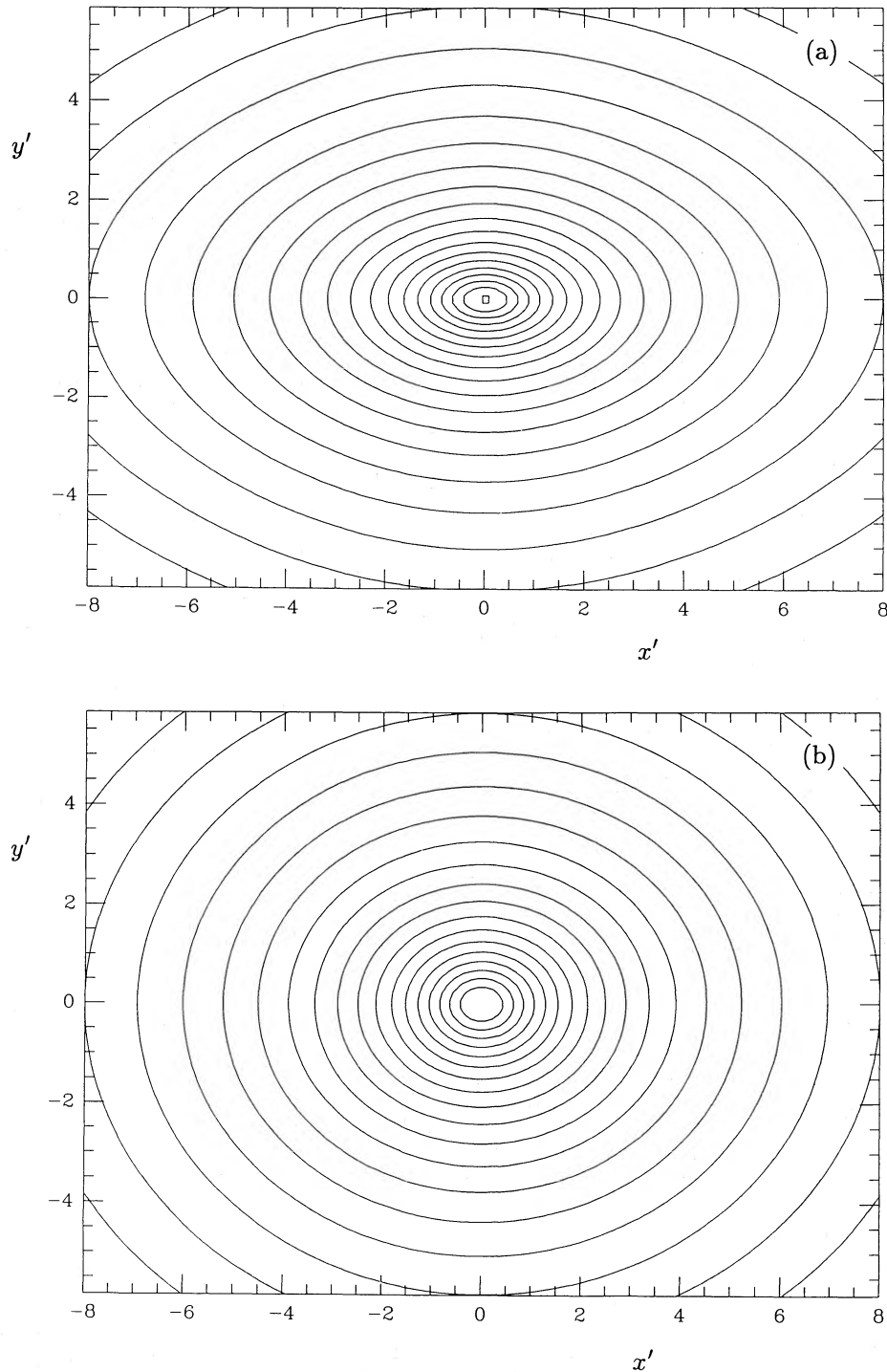


FIG. 11.—Projected surface density of oblate and prolate Kuzmin-Kutuzov models for two values of the viewing angle θ with respect to the z -axis. (a) $c/a = 0.5$, $\theta = 90^\circ$. (b) $c/a = 0.5$, $\theta = 45^\circ$. (c) $c/a = 1.25$, $\theta = 90^\circ$. (d) $c/a = 1.25$, $\theta = 45^\circ$.

We can freely choose a function of three variables in the construction of a three-integral distribution function that corresponds to a given mass density. Therefore, it would be quite impractical to discuss the resulting model space in any detail. Instead, we chose to give a few examples which (a) show how these fully self-consistent models can be constructed, and (b) illustrate the effects of triaxial velocity distributions on various observable properties. The examples of § Vb show that use of three-integral models with positive distribution functions does make a difference in the analysis of kinematic data.

That our modified Fricke method is capable of producing explicit distribution functions $F(E, I_2, I_3)$ for the Kuzmin-Kutuzov model is due to the fortunate circumstance that for this model the complete density ρ , as well as each of the components ρ_{lmn} , can be written explicitly as a function of ϖ and ψ , so that the two-integral inversion can be done in closed form. It is very likely that other

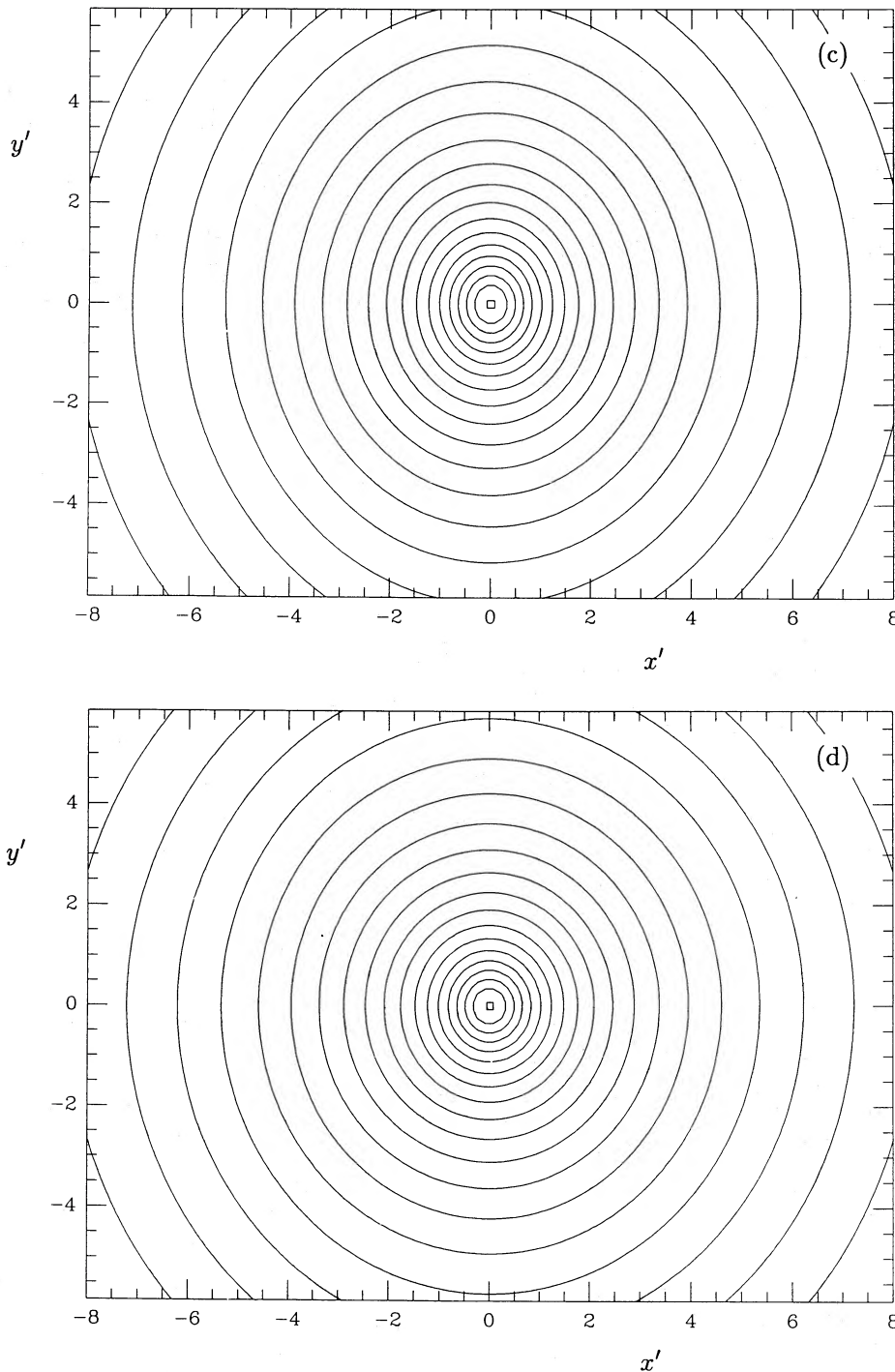


FIG. 11.—Continued

models with this property exist. One way to search for them in a systematic fashion could be to use the generating function method outlined in D86 to construct models with $\rho = \rho(\varpi, \psi)$, and then to ask for which of these the potential ψ is of Stäckel form.

Instead of using $F(E, I_2)$ to represent the remaining density, as we have done here, we could also have used the simpler inversion formula for the representation of a given axisymmetric density in a Stäckel potential by infinitesimally thin tube orbits only (Bishop 1987; de Zeeuw 1988; Hunter *et al.* 1988). The advantage of this approach is that it requires only a one-dimensional quadrature, and applies to any axisymmetric Stäckel potential. In the equivalent spherical models, the remaining density is represented by stars on circular orbits. The disadvantage of using the thin orbit distribution functions is that they are rather special, and contain a δ -function. However, the example of the Galactic halo shows that models with a substantial fraction of stars on tube orbits with a small radial extent are useful (White 1985; Levison and Richstone 1986; Dejonghe and de Zeeuw 1988). The thin orbit distribution

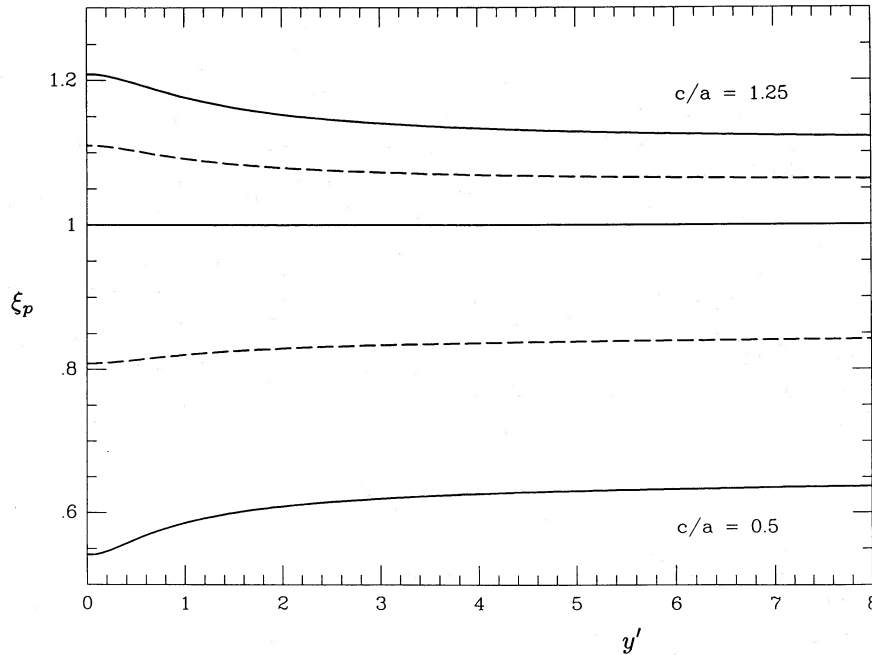


FIG. 12.—Apparent axis ratio ξ_p of the contours of projected surface density as function of the distance y' along the projected z -axis for the models of Fig. 11. Two inclinations are shown: $\theta = 90^\circ$ (full curves) and $\theta = 45^\circ$ (dashed curves).

function for the density distribution of the Kuzmin-Kutuzov model can be expressed in terms of elementary functions (de Zeeuw 1988). Whether this is true also for individual components ρ_{lmn} remains to be seen.

For the construction of models of observed galaxies, we suspect that it is probably most efficient to take a limited number of components F_{lmn} , and fit the corresponding density components to a given density, e.g., by a least-squares method. Furthermore, since all the velocity moments of the components can be calculated as well, one can fit density and velocity information simultaneously. This can be done directly for the projected quantities. As already mentioned in § IIIb, we do not have to limit ourselves to components of the form given in equation (3.13). The inversion method of Dejonghe (1988) can be used to specify more general components. It should be noted that the numerical fitting approach can be used also in the spherical case. Work along these lines is in progress.

b) Triaxial Stäckel Models

The density $\rho_{lmn}(x, y, z)$ that corresponds to a distribution function $F_{lmn}(E, I_2, I_3) = E^l I_2^m (p + qE + rI_2 + 2sI_3)^n$ in a triaxial Stäckel potential is given by an integral of the form (3.6), but with the I_2 integration over an interval $[I_2^-, I_2^+]$ with $I_2^- \neq 0$. We expect that the change in integration limits will not complicate the evaluation of the integral significantly, so that ρ_{lmn} can be calculated explicitly by means of the methods of Appendix A. It follows that Fricke's method generalizes to triaxial models as well. The construction of exact models in this way will again be limited by the cumbersome form of the individual components.

Application of our modified version of the Fricke method in order to obtain exact triaxial models requires an inversion formula that produces the distribution function of the density that remains after subtraction of the part contributed by the chosen components ρ_{lmn} . Dejonghe (1988) has derived such an inversion formula, but with the caveat that one has to specify the remaining density in a form $\rho(\lambda, \mu, \nu, U, V, W)$, where $U, V,$ and W each are functions of $\lambda, \mu,$ and ν that must satisfy certain compatibility conditions.

Triaxial Stäckel models also allow thin orbit solutions. However, in this case part of the density must be reproduced by box orbits, and their distribution function is the solution of a Volterra integral equation of the first kind in three variables, which has to be solved by numerical means (de Zeeuw, Hunter, and Schwarzschild 1987; Hunter 1987).

It is evident that the fitting method proposed in § VIa can be applied to triaxial Stäckel models as well.

c) Concluding Remark

The subject of stability of equilibrium models has recently become an area of active research (Fridman and Polyachenko 1984; Merritt 1987). Since few analytic results are available, even in the spherical case, the stability of a given dynamical model is usually tested by means of N -body schemes. The existing nonspherical dynamical models have been constructed by linear programming or an equivalent method, on a grid of cells in configuration space that is of necessity rather coarse (e.g., Statler 1987). Use of these models in order to set up the smooth initial conditions required for a stability determination with a numerical N -body program is therefore difficult. The method presented here, and its intended generalization to triaxial models, yields smooth distribution functions by design. We expect that the resulting models will be more amenable to numerical stability analysis than previous ones.

The hospitality of the Canadian Institute for Theoretical Astrophysics, where some of the calculations reported here were performed, is gratefully acknowledged. This research was supported in part by High Technology Grant NJS 88-240090-2, and by an RCA Fellowship to T. d. Z.

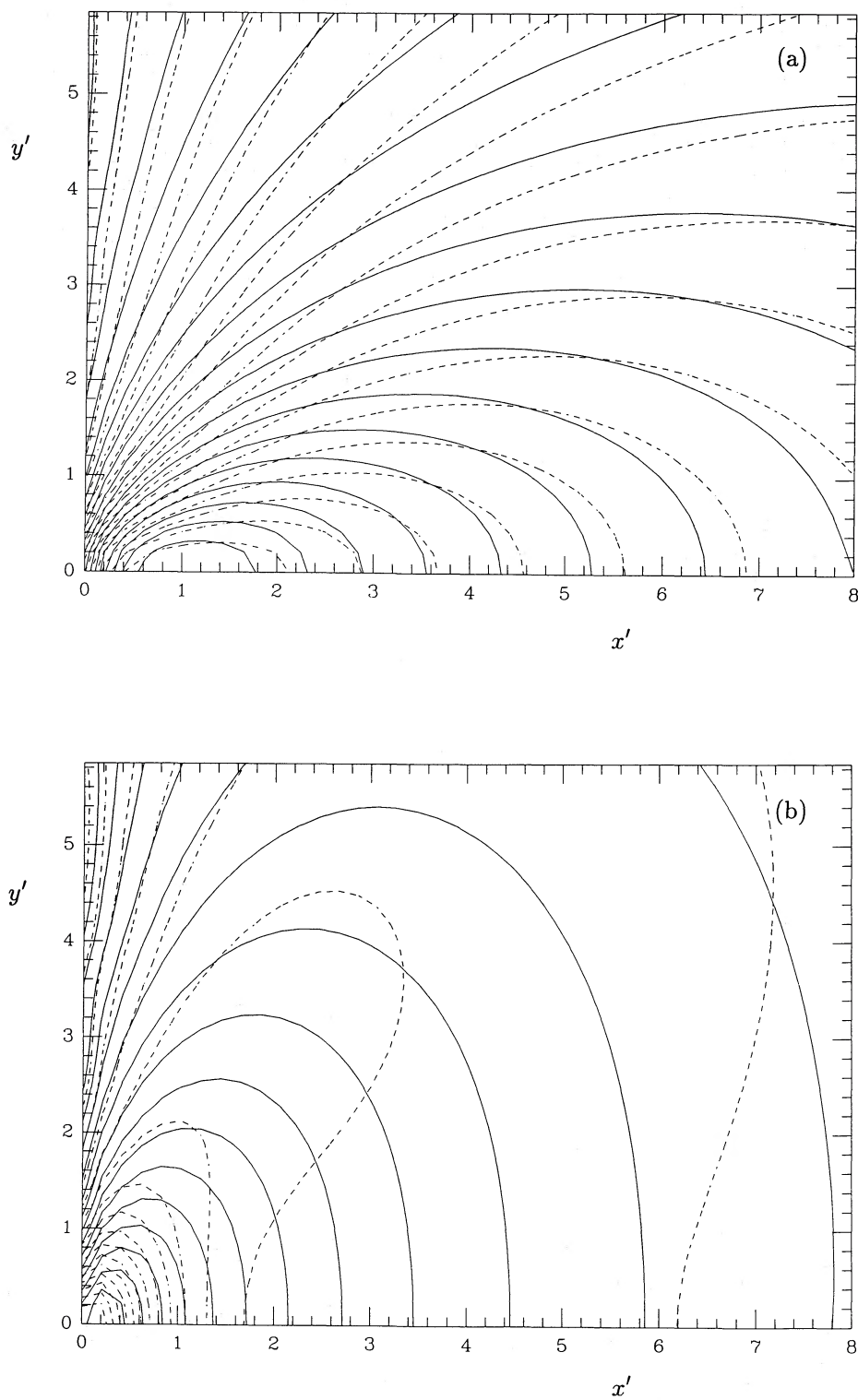


FIG. 13.—The radial velocity field observed at $\theta = 90^\circ$ for the maximum streaming models with $F = F(E, L_z^2)$ (full curves) and with the three-integral distribution function of Figs. 9 and 10 (dashed curves). (a) $c/a = 0.5$. (b) $c/a = 1.25$.

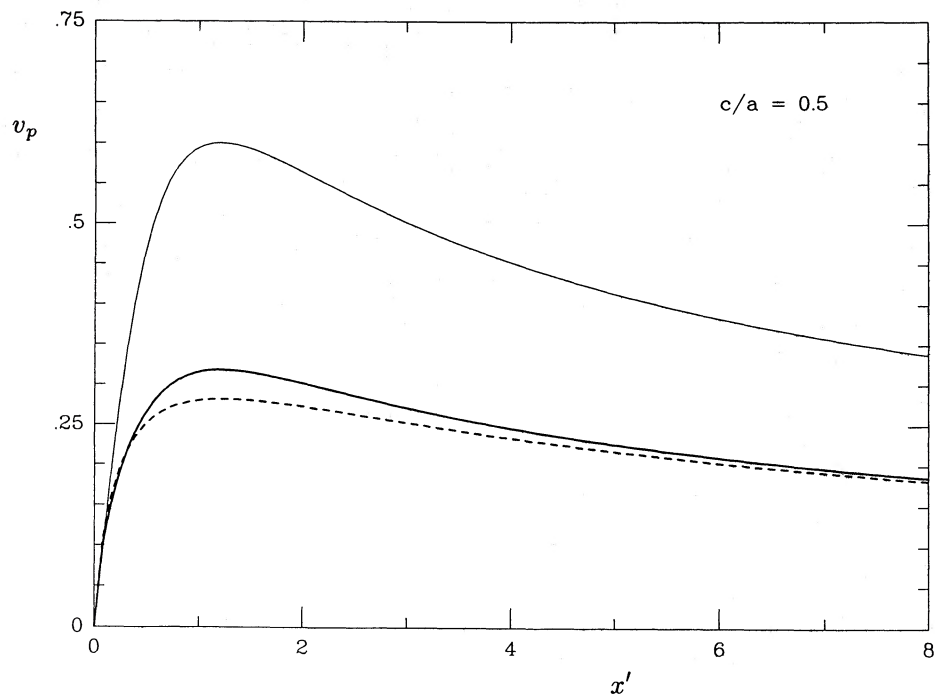


FIG. 14a

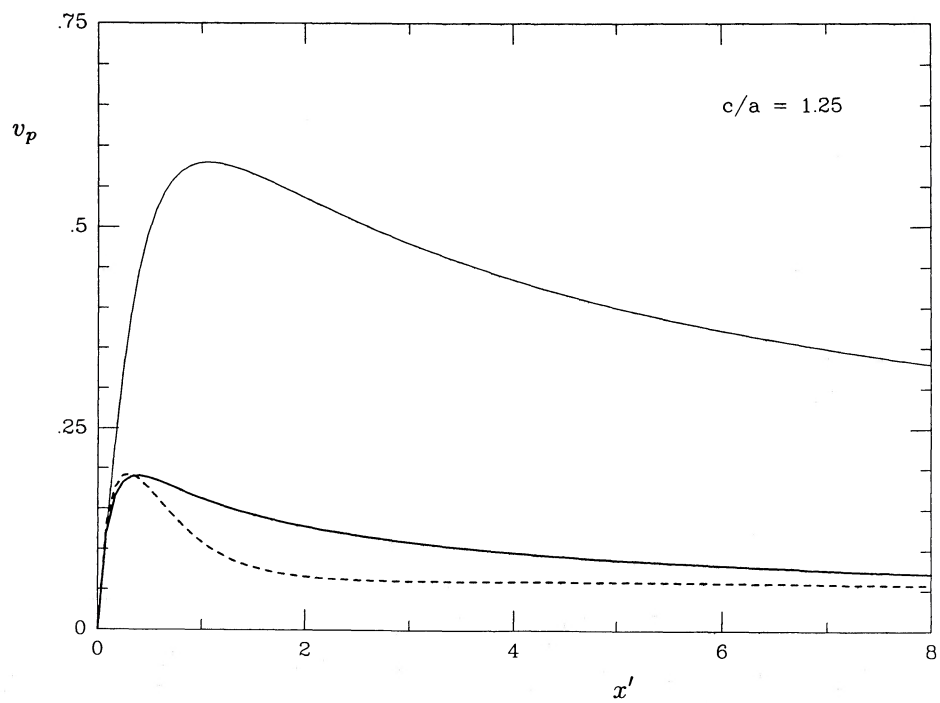


FIG. 14b

FIG. 14.—Projected equatorial radial velocity of the models of Fig. 13 with $c/a = 0.5$ and $c/a = 1.25$, for a viewing angle $\theta = 90^\circ$. Curves are shown for $F = F(E, L^2)$ (solid) and also for the three-integral distribution function considered in the text (dashed), with all stars rotating in the same direction. Upper curve is the circular velocity profile.

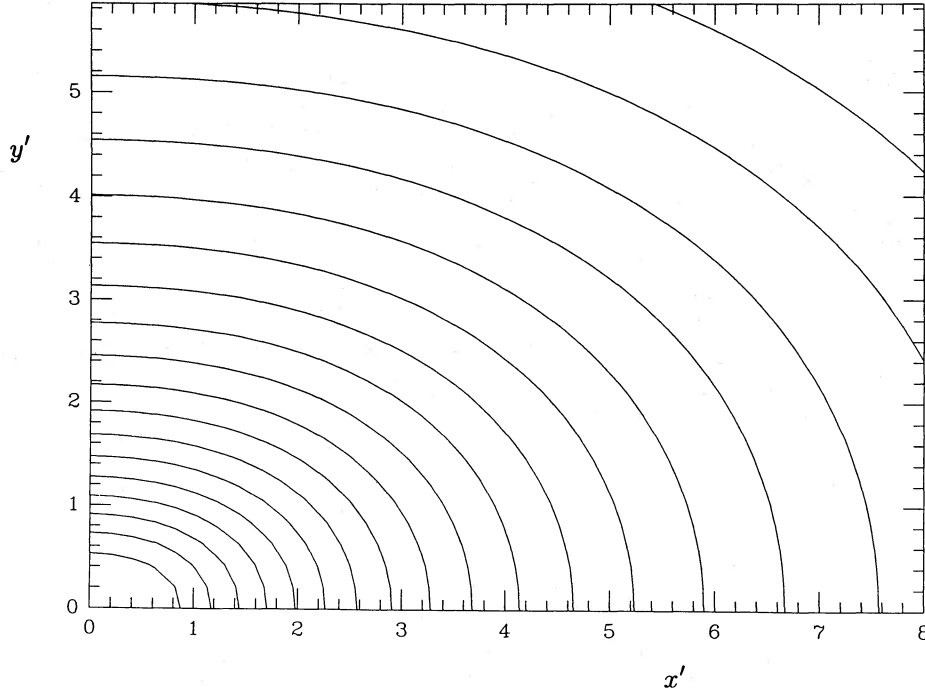


FIG. 15.—Projected velocity dispersion field for $\theta = 90^\circ$ for the oblate two-integral model with isotropic spatial velocity dispersions

APPENDIX A

THE DENSITY CORRESPONDING TO $F = E^l I_2^m (p + qE + rI_2 + 2sI_3)^n$

In this appendix we evaluate the fundamental integral (3.2), in order to find the density that corresponds to the distribution function $F = E^l I_2^m (p + qE + rI_2 + 2sI_3)^n$. We employ several formulae that are given, e.g., in Gradshteyn and Ryzhik (1980, hereafter GR).

For this choice of F , the integral (3.6) can be written as

$$\rho_{lmn} = \frac{2\sqrt{2}}{\varpi} \int_0^\psi E^l dE \int_0^{I_2^+} I_2^{m-1/2} dI_2 \int_{I_3^-}^{I_3^+} \frac{(p + qE + rI_2 + 2sI_3)^n dI_3}{\sqrt{(I_3^+ - I_3)(I_3 - I_3^-)}}, \quad (\text{A1})$$

where the integration limits are given in equations (3.4) and (3.5). We first consider the integral over I_3 ,

$$J_3 = \int_{I_3^-}^{I_3^+} (p + qE + rI_2 + 2sI_3)^n \frac{dI_3}{\sqrt{(I_3^+ - I_3)(I_3 - I_3^-)}}. \quad (\text{A2})$$

By means of GR (eq. [3.197.3]) we find

$$J_3 = (p + qE + rI_2 + 2sI_3^-)^n \pi {}_2F_1\left(-n, \frac{1}{2}; 1; -2s \frac{I_3^+ - I_3^-}{p + qE + rI_2 + 2sI_3^-}\right), \quad (\text{A3})$$

where ${}_2F_1$ is the standard hypergeometric function. This expression shows no apparent symmetry in λ and ν , although it follows from inspection of the integral (A2) that there should be. Application of the following quadratic transformation on the hypergeometric function, given in GR (eq. [9.134.1]),

$${}_2F_1\left(-n, \frac{1}{2}; 1; z\right) = \left(1 - \frac{z}{2}\right)^n {}_2F_1\left[-\frac{n}{2}, -\frac{n-1}{2}; 1; \left(\frac{z}{2-z}\right)^2\right], \quad (\text{A4})$$

makes this symmetry transparent; we obtain

$$J_3 = [p + qE + rI_2 + s(I_3^+ + I_3^-)]^n \pi {}_2F_1\left(-\frac{n}{2}, -\frac{n-1}{2}; 1; \frac{[s(I_3^+ - I_3^-)]^2}{[p + qE + rI_2 + s(I_3^+ + I_3^-)]^2}\right). \quad (\text{A5})$$

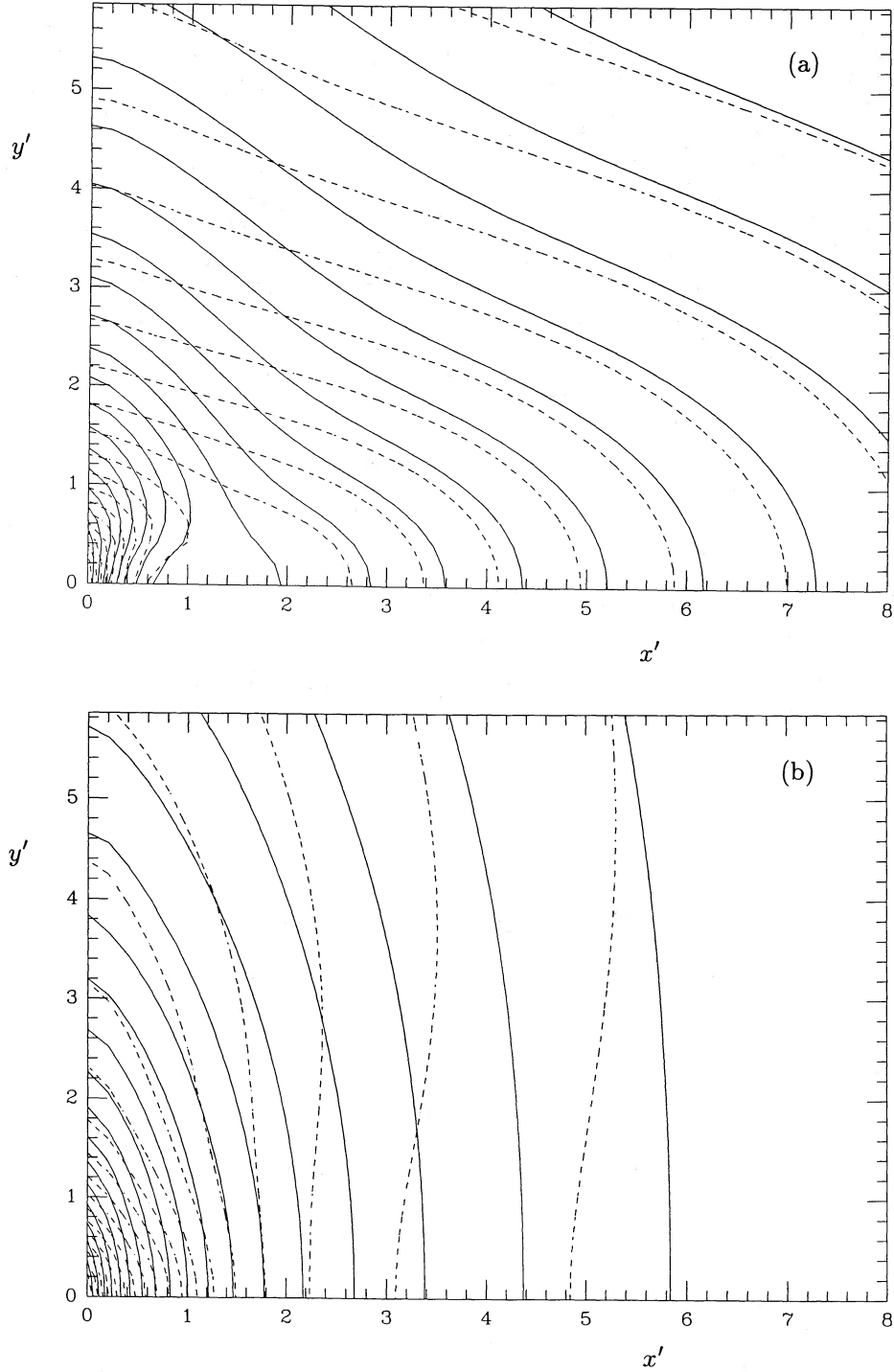


FIG. 16.—Projected velocity dispersion field for $\theta = 90^\circ$ for the oblate and prolate Kuzmin-Kutuzov models and the distribution functions of Fig. 13

Since n is an integer, the hypergeometric function is a finite series, and we find for equation (A5), after some rearrangements of terms

$$J_3 = \pi \sum_{i=0}^{n/2} \frac{(-n)_{2i}}{(i!)^2} [(p + sA) + (q - sB)E + (r + sC)I_2]^{n-2i} 2^{-2i} s^{2i} \left[\frac{(\lambda - \nu)(\gamma - \alpha)}{(\lambda + \alpha)(\nu + \alpha)} \right]^{2i} (I_2^+ - I_2)^{2i}, \quad (\text{A6})$$

where we have used (see eqs. [3.4] and [3.5])

$$I_3^+ - I_3^- = \frac{(\lambda - \nu)(\alpha - \gamma)}{(\lambda + \alpha)(\nu + \alpha)} (I_2^+ - I_2), \quad (\text{A7})$$

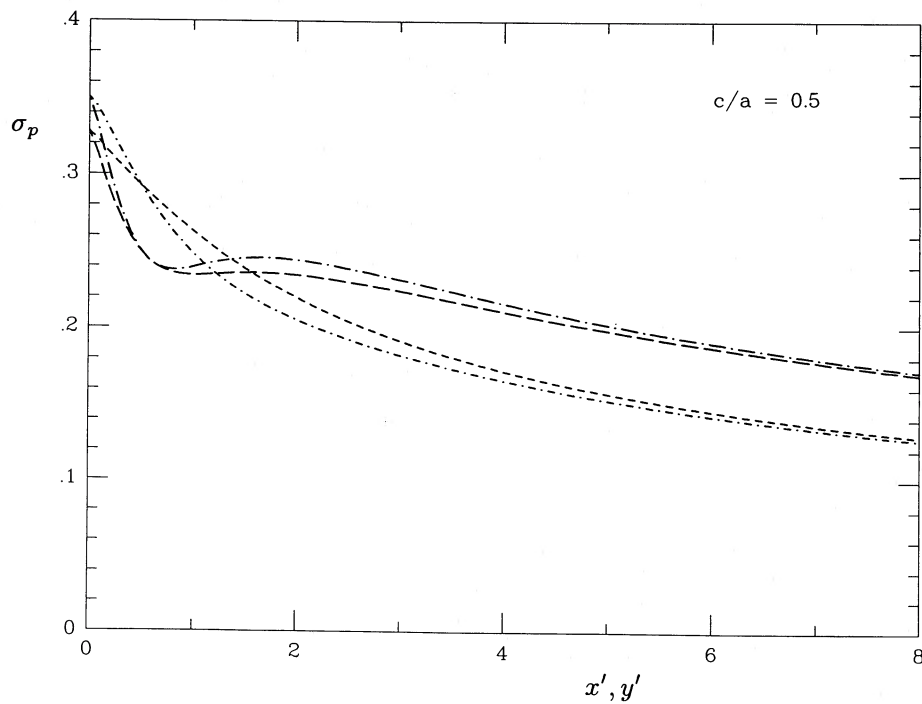


FIG. 17a

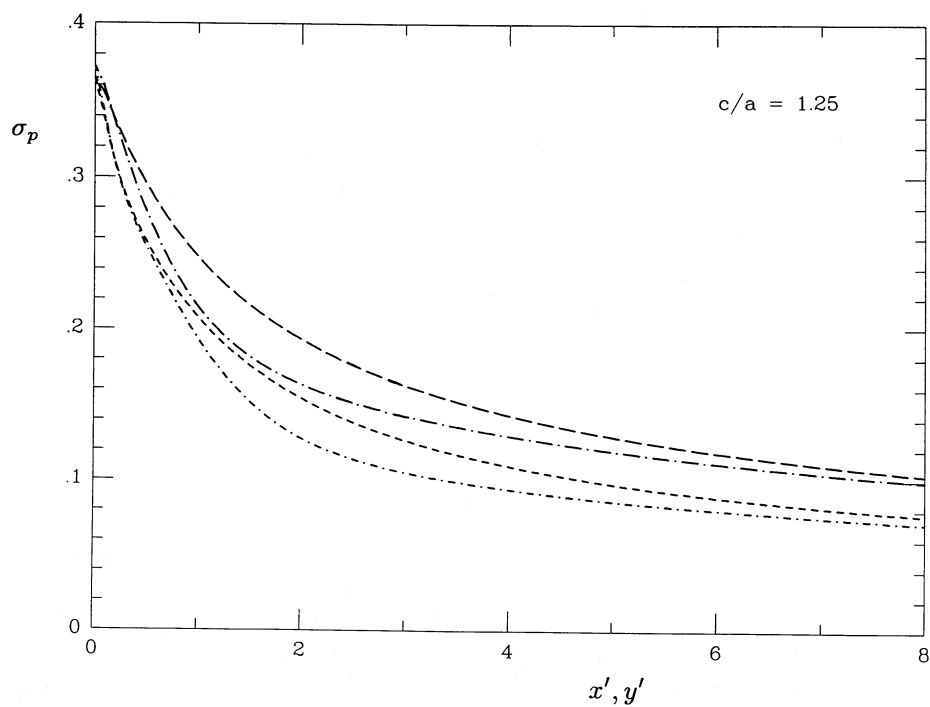


FIG. 17b

FIG. 17.—Projected velocity dispersions, as observed along the major and the minor axis for the models of Fig. 13. Dashed curves are for $F(E, L_2)$, and the dot-dash curves are for $F(E, L_2^2, I_3)$. The major axis profiles are drawn with long dashes, and the minor axis profiles have short dashes.

and

$$I_3^+ + I_3^- = A - BE + CI_2, \tag{A8}$$

with

$$A = f(\lambda) + f(v), \quad B = \lambda + v + 2\gamma, \quad C = -\frac{(\lambda + v)(\gamma + \alpha) + 2(\lambda v + \alpha\gamma)}{(\lambda + \alpha)(v + \alpha)}. \tag{A9}$$

Upon substitution of equation (A9), the integration over I_2 can be written as

$$J_2 = \int_0^{I_2^+} I_2^{m-1/2} (I_2^+ - I_2)^{2i} (A' + B'E + C'I_2)^{n-2i} dI_2, \tag{A10}$$

where we have defined

$$A' = p + sA, \quad B' = q - sB, \quad C' = r + sC. \tag{A11}$$

Binomial expansion of the first term in brackets in equation (A6), and use of GR (eq. [3.191.3]) and equation (3.5) then gives

$$J_2 = \sum_{j=0}^{n-2i} \binom{n-2i}{j} C'^j B \left(m + \frac{1}{2} + j, 2i + 1\right) \varpi^{2m+1+4i+2j} (A' + B'E)^{n-2i-j} (\psi - E)^{m+2i+j+1/2}. \tag{A12}$$

Finally, we are left with the evaluation of

$$\begin{aligned} \rho_{lmn} &= \frac{2^{3/2}\pi}{\varpi} \sum_{i=0}^{n/2} \frac{(2i)!(-n)_{2i}}{(i!)^2 2^{2i}} s^{2i} (\lambda - v)^{2i} \sum_{j=0}^{n-2i} \binom{n-2i}{j} C'^j \frac{\Gamma(m + 1/2 + j)}{\Gamma(m + 3/2 + j + 2i)} \\ &\times \varpi^{2m+1+2j} \int_0^\psi E^l (A' + B'E)^{n-2i-j} (\psi - E)^{m+2i+j+1/2} dE. \end{aligned} \tag{A13}$$

We first rename the indices, and write $k = 2i + j$. This results in

$$\begin{aligned} \rho_{lmn} &= 2^{3/2} \sqrt{\pi} n! \varpi^{2m} \sum_{k=0}^n \frac{1}{\Gamma(n + 1 - k) \Gamma(m + 3/2 + k)} \\ &\times \sum_{i=0}^{k/2} \frac{\Gamma(i + 1/2) \Gamma(m + 1/2 + k - 2i)}{i!(k - 2i)!} s^{2i} (\lambda - v)^{2i} C'^k \varpi^{2k-4i} \int_0^\psi E^l (A' + B'E)^{n-k} (\psi - E)^{m+1/2+k} dE. \end{aligned} \tag{A14}$$

Subsequently we evaluate the integral, after binomial expansion of the term $(A' + B'E)^{n-k}$ and use of GR (eq. [3.191.3]). This gives

$$\begin{aligned} \rho_{lmn} &= 2^{3/2} \sqrt{\pi} l! n! \varpi^{2m} \sum_{k=0}^n \frac{1}{\Gamma(m + 3/2 + k)} \sum_{i=0}^{k/2} \frac{\Gamma(i + 1/2) \Gamma(m + 1/2 + k - 2i)}{i!(k - 2i)!} s^{2i} (\lambda - v)^{2i} C'^k \varpi^{2k-4i} \\ &\times \sum_{j=0}^{n-k} \frac{\Gamma(m + n + 3/2 - j)}{\Gamma(l + m + n + 5/2 - j) j! (n - k - j)!} (A' + B'\psi)^j (-B')^{n-j-k} \psi^{l+m+n+3/2-j}. \end{aligned} \tag{A15}$$

This is the density that corresponds to a distribution function $F = E^l I_2^m (p + qE + rI_2 + 2sI_3)^n$ and an axisymmetric Stäckel potential ψ .

APPENDIX B

THE MOMENTS OF $F = E^l I_2^m (p + qE + rI_2 + 2sI_3)^n$

The unnormalized velocity moments of $F(E, L_z, I_3)$ in spheroidal coordinates (λ, ϕ, v) are defined in equation (3.23). After transformation of variables from the velocities $v_\lambda, v_\phi,$ and v_v to $E, I_2,$ and I_3 , the resulting triple integration is quite similar to the one obtained for the mass density, which is a special case of equation (3.23) for $\rho = \sigma = \tau = 0$. In contrast with Appendix A, we do not have to account for a symmetry in λ and v , since this symmetry only occurs when $\rho = \tau$.

I. THE EVEN MOMENTS

We first consider the case where $\rho, \sigma,$ and τ are all even. This means we have to evaluate

$$\mu_{2\rho, 2\sigma, 2\tau} = \frac{2^{\rho+\sigma+\tau+3/2}}{(\lambda - v)^{\rho+\tau} \varpi^{2\sigma+1}} \int_0^\psi E^l dE \int_0^{I_2^+} I_2^{m+\sigma-1/2} dI_2 \int_{I_3^-}^{I_3^+} (p + qE + rI_2 + 2sI_3)^n (I_3^+ - I_3)^{\rho-1/2} (I_3 - I_3^-)^{\tau-1/2} dI_3. \tag{B1}$$

The integration over $I_3,$

$$\int_{I_3^-}^{I_3^+} (p + qE + rI_2 + 2sI_3)^n (I_3^+ - I_3)^{\rho-1/2} (I_3 - I_3^-)^{\tau-1/2} dI_3, \tag{B2}$$

can be done by means of GR (eq. [3.197.3]). Just as for the case $\rho = \sigma = \tau = 0$, discussed in Appendix A, this yields a hypergeometric function the series for which terminates. As a result, the integral (B2) can be written as

$$(I_3^+ - I_3^-)^{\rho+\tau} \sum_{i=0}^n \binom{n}{i} \frac{\Gamma(\tau+i+1/2)\Gamma(\rho+1/2)}{\Gamma(\rho+\tau+i+1)} s^i (p+qE+rI_2+sI_3^-)^{n-i} (I_3^+ - I_3^-)^i. \quad (\text{B3})$$

After substitution of equation (B3) into equation (B1), and expression of I_3^- and $I_3^+ - I_3^-$ in terms of E, I_2, λ , and ν by means of equations (3.4) and (A7), we are left with

$$\begin{aligned} \mu_{2\rho, 2\sigma, 2\tau} &= \frac{2^{\rho+\sigma+\tau+3/2}}{\varpi^{2\rho+2\sigma+2\tau+1}} \int_0^\psi E^l dE \sum_{i=0}^n \binom{n}{i} s^i \frac{\Gamma(\tau+i+1/2)\Gamma(\rho+1/2)}{\Gamma(\rho+\tau+i+1)} \frac{(\lambda-\nu)^i}{\varpi^{2i}} \\ &\times \int_0^{I_2^i} \left\{ p + s(\nu+\gamma)G(\nu) + [q - s(\nu+\gamma)]E + \left(r - s \frac{\nu+\gamma}{\nu+\alpha} \right) I_2 \right\}^{n-i} (I_2^+ - I_2)^{\rho+\tau+i} I_2^{\sigma-1/2} dI_2. \end{aligned} \quad (\text{B4})$$

Upon binomial expansion of the term in braces, the integral over I_2 can be evaluated with the help of GR (eq. [3.191.3]):

$$\begin{aligned} \mu_{2\rho, 2\sigma, 2\tau} &= 2^{\rho+\sigma+\tau+3/2} \varpi^{2m} \Gamma\left(\rho + \frac{1}{2}\right) \int_0^\psi E^l (\psi - E)^{\rho+\sigma+\tau+m+i+j+1/2} dE \\ &\times \sum_{i=0}^n \binom{n}{i} s^i \Gamma\left(\tau + i + \frac{1}{2}\right) \frac{(\lambda-\nu)^i}{\varpi^{2i}} \sum_{j=0}^{n-i} \binom{n-i}{j} \frac{\Gamma(m+\sigma+j+1/2)}{\Gamma(\rho+\sigma+\tau+m+i+j+3/2)} \\ &\times \{ p + s(\nu+\gamma)G(\nu) + [q - s(\nu+\gamma)]E \}^{n-i-j} \left(r - s \frac{\nu+\gamma}{\nu+\alpha} \right)^j \varpi^{2(i+j)}. \end{aligned} \quad (\text{B5})$$

After a similar expansion of the term in braces in equation (B5) we finally obtain

$$\begin{aligned} \mu_{2\rho, 2\sigma, 2\tau} &= 2^{\rho+\sigma+\tau+3/2} \varpi^{2m} \psi^{\rho+\sigma+\tau+l+m+3/2} \Gamma\left(\rho + \frac{1}{2}\right) \\ &\times \sum_{i=0}^n \binom{n}{i} s^i \Gamma\left(\tau + i + \frac{1}{2}\right) (\lambda-\nu)^i \sum_{j=0}^{n-i} \binom{n-i}{j} \Gamma\left(m+\sigma+j+\frac{1}{2}\right) \left(r - s \frac{\nu+\gamma}{\nu+\alpha} \right)^j \varpi^{2j} \\ &\times \sum_{k=0}^{n-i-j} \binom{n-i-j}{k} \frac{\Gamma(k+l+1)}{\Gamma(\rho+\sigma+\tau+l+m+i+j+k+5/2)} [p + s(\nu+\gamma)G(\nu)]^{n-i-j-k} [q - s(\nu+\gamma)]^k \psi^{i+j+k}. \end{aligned} \quad (\text{B6})$$

We remark that for $\rho = \tau$ this expression can be written in a form that is manifest symmetric in λ and ν by a transformation similar to that used in Appendix A. For the special case $\rho = \tau = 0$ the resulting expression can be obtained from equation (A15) by substitution of $m + \sigma$ for m , and multiplication by $[\varpi\sqrt{2}]^{2\sigma}$.

II. THE ODD MOMENTS

By symmetry, $\mu_{2\rho+1, \sigma, \tau} = \mu_{2\rho, \sigma, 2\tau+1} = 0$, so that we only have to consider $\mu_{2\rho, \sigma, 2\tau}$. As pointed out in § IIIa, we are interested only in the case with no net rotation, and the case of maximum rotation. For the former we find $\mu_{2\rho, 2\sigma+1, 2\tau} = 0$, and for the latter we obtain (see eq. [3.9])

$$\mu_{2\rho, 2(\sigma+1/2), 2\tau}^{\pm} = \frac{1}{2} \mu_{2\rho, 2(\sigma+1/2), 2\tau}, \quad (\text{B7})$$

where $\mu_{2\rho, 2\sigma+1, 2\tau}$ is given by equation (B6).

APPENDIX C

THE COMPONENT $\rho = \psi^p \varpi^{2q} (1 - A\varpi^2 \psi^2)^r$

In this Appendix we collect some properties of the two-integral model with $F = F(E, L_z^2)$ that is consistent with a mass density of the form $\rho = \psi^p \varpi^{2q} (1 - A\varpi^2 \psi^2)^r$. They can be derived by a straightforward application of the general theory given in D86.

The distribution function $F(E, L_z^2)$ is given by

$$F(E, L_z) = \frac{1}{2^{3/2} \pi} \frac{\Gamma(p+1)}{\Gamma(q+1/2)\Gamma(p-1/2-q)} E^{p-q-3/2} I_2^q {}_3F_2\left(\frac{p+1}{2}, \frac{p}{2}+1, -r; p-q-\frac{1}{2}, q+\frac{1}{2}; 2AEL_z^2\right), \quad (\text{C1})$$

where ${}_3F_2$ is a generalized hypergeometric function (see eq. [4.23]). In the special cases with either $r = 0$ or $q = 0$ we recover the results already obtained by D86 (eqs. [2.5.48] and [2.5.54]).

The nontrivial velocity moments $\mu_{2i, m, 2j}$, defined as

$$\mu_{2i, m, 2j} = \iiint F(E, L_z) v_\varpi^{2i} v_\phi^m v_z^{2j} dv_\varpi dv_\phi dv_z, \quad (\text{C2})$$

can be written concisely as

$$\mu_{2i,m,2j} = \frac{1}{\pi} B\left(i + \frac{1}{2}, j + \frac{1}{2}\right) \mu_{2(i+j),m}, \quad (\text{C3})$$

where $B(s, t)$ is the Beta function, and the simplified moments $\mu_{2(i+j),m}$ are given by

$$\begin{aligned} \mu_{2n,m} &= 2^{n+m/2} \Gamma(n+1) \frac{\Gamma[q + (m+1)/2]}{\Gamma(q+1/2)} \frac{\Gamma(p+1)}{\Gamma(p+1+n+m/2)} \psi^{p+n+m/2} \varpi^{2q} \\ &\times {}_4F_3\left(-r, q + \frac{m+1}{2}, \frac{p+1}{2}, \frac{p}{2} + 1; q + \frac{1}{2}, \frac{p+1+n+m/2}{2}, \frac{p+n+m/2}{2} + 1, A\varpi^2\psi^2\right), \end{aligned} \quad (\text{C4})$$

and ${}_4F_3$ is a generalized hypergeometric function. The remaining moments are all zero. For odd values of m , expression (C4) refers to the case where all stars are orbiting in a counterclockwise direction. In case they all orbit in the opposite direction the odd moments should be multiplied by minus one. We conclude that it is possible to express all the velocity moments explicitly in terms of ϖ and ψ .

One can verify easily that for $n = m = 0$ equation (C4) produces the mass density. The case $m = 1, n = 0$ gives the maximum mean streaming velocity

$$\rho \langle v_\phi^\pm \rangle = \pm \sqrt{2} \frac{\Gamma(q+1)}{\Gamma(q+1/2)} \frac{\Gamma(p+1)}{\Gamma(p+3/2)} \psi^{p+1/2} \varpi^{2q} {}_4F_3\left(-r, q+1, \frac{p+1}{2}, \frac{p}{2} + 1; q + \frac{1}{2}, \frac{p}{2} + \frac{3}{4}, \frac{p}{2} + \frac{5}{4}, A\varpi^2\psi^2\right). \quad (\text{C5})$$

The velocity dispersions follow from

$$\begin{aligned} \rho \sigma_\varpi^2 &= \rho \sigma_z^2 = \frac{1}{p+1} \psi^{p+1} \varpi^{2q} {}_2F_1\left(-r, \frac{p+1}{2}; \frac{p+3}{2}, A\varpi^2\psi^2\right), \\ \rho(\sigma_\phi^2 + \langle v_\phi \rangle^2) &= \frac{2q+1}{p+1} \psi^{p+1} \varpi^{2q} {}_3F_2\left(-r, q + \frac{3}{2}, \frac{p+1}{2}; q + \frac{1}{2}, \frac{p+3}{2}, A\varpi^2\psi^2\right) \\ &= (2q+1) \rho \sigma_\varpi^2 - \frac{2rA}{p+3} \psi^{p+3} \varpi^{2q+2} {}_2F_1\left(1-r, \frac{p+3}{2}; \frac{p+5}{2}, A\varpi^2\psi^2\right). \end{aligned} \quad (\text{C6})$$

We remark that none of the above formulae converge when $A\varpi^2\psi^2 \leq -1$, which may occur in the prolate case. However, the analytic continuation of the distribution function given in equation (C1) can be obtained in the same way as in § IVc. When $q = 0$ this is trivial. The case in which q is a positive integer can be reduced to a sum of cases with $q = 0$.

Rather than embarking on the circuitous route of getting the analytic continuation of the moments directly from the (generalized) hypergeometric functions, we note that, if necessary, the moments can always be calculated from equation (C2) and the analytic continuation of (C1).

APPENDIX D

THE JEANS EQUATIONS

The Jeans equations for an axisymmetric density ρ in a potential ψ that is of Stäckel form in spheroidal coordinates (λ, ϕ, ν) are given by (Lynden-Bell 1960)

$$\begin{aligned} \frac{\partial T_\lambda}{\partial \lambda} + \frac{T_\lambda - T_\phi}{2(\lambda + \alpha)} + \frac{T_\lambda - T_\nu}{2(\lambda - \nu)} &= \rho \frac{\partial \psi}{\partial \lambda}, \\ \frac{\partial T_\nu}{\partial \nu} + \frac{T_\nu - T_\lambda}{2(\nu - \lambda)} + \frac{T_\nu - T_\phi}{2(\nu + \alpha)} &= \rho \frac{\partial \psi}{\partial \nu}, \end{aligned} \quad (\text{D1})$$

where we have written $T_\tau = \rho \langle v_\tau^2 \rangle$, with $\tau = \lambda, \phi$, or ν . Elimination of T_ϕ gives an equation in T_λ and T_ν only:

$$(\lambda + \alpha) \frac{\partial T_\lambda}{\partial \lambda} - (\nu + \alpha) \frac{\partial T_\nu}{\partial \nu} + T_\lambda - T_\nu = \rho(\lambda + \alpha) \frac{\partial \psi}{\partial \lambda} - \rho(\nu + \alpha) \frac{\partial \psi}{\partial \nu} = \Psi(\lambda, \nu). \quad (\text{D2})$$

This equation is a linear partial differential equation of the first order. It is of a form similar to the equation derived by Bacon (1985) in his study of general axisymmetric models in which the velocity dispersion tensor is aligned in spherical coordinates. By a suitable definition of variables equation (D2) becomes identical to the one solved by Bacon.

Following Bacon, we introduce the anisotropy parameter $\beta(\lambda, \nu)$ as

$$\beta(\lambda, \nu) = 1 - \frac{T_\nu}{T_\lambda} = 1 - \frac{\sigma_\nu^2}{\sigma_\lambda^2}, \quad (\text{D3})$$

and define the auxiliary quantities

$$g(\lambda) = \ln(\lambda + \alpha), \quad h(v) = -\ln|v + \alpha|, \quad \Lambda(\lambda, v) = -\beta + \frac{\partial\beta}{\partial h}. \quad (\text{D4})$$

In these variables, equation (D2) reduces to the standard form

$$\frac{\partial T_\lambda}{\partial g} + \text{sign}(\gamma - \alpha)(1 - \beta) \frac{\partial T_\lambda}{\partial h} = \Lambda T_\lambda + \Psi. \quad (\text{D5})$$

The general solution, subject to the boundary condition $T_\lambda \rightarrow 0$ for $\lambda \rightarrow +\infty$, is given by Bacon as

$$T_\lambda(g, h) = - \int_g^{+\infty} du \Psi\{u, H[\Phi(g, h), u]\} \exp \left[\int_u^g dv \Lambda\{v, H[\Phi(g, h), v]\} \right]. \quad (\text{D6})$$

Here the integrations are along the characteristics given by

$$\frac{dh}{dg} = \text{sign}(\gamma - \alpha)(1 - \beta), \quad (\text{D7})$$

so that

$$h = H(C, g), \quad C = \Phi(g, h). \quad (\text{D8})$$

Any choice of $\beta(\lambda, v)$ will give us the characteristics, so that T_λ can be evaluated via equation (D6). The value of T_v subsequently follows from the definition of β , and T_ϕ can be calculated from either one of equations (D1).

It follows immediately from the form (D1) of the Jeans equations that for any nonsingular solution the functions T_λ , T_ϕ , and T_v have the same value at the foci, i.e.,

$$T_\lambda(-\alpha, -\alpha) = T_\phi(-\alpha, -\alpha) = T_v(-\alpha, -\alpha), \quad (\text{D9})$$

so that we must have $\beta(-\alpha, -\alpha) = 0$.

For $\beta = 0$ everywhere, we have $T_\lambda = T_v$, so that the velocity distribution is isotropic in the meridional plane. This is the case where $F = F(E, I_2)$, and the general solution can be written in the form given in equation (3.32). For the special solutions in which all stars are on infinitesimally thin tube orbits the velocity dispersions are given by similar simple quadratures (de Zeeuw 1988; Hunter *et al.* 1988). These correspond to the limiting forms of the general solution obtained for $\beta \rightarrow -\infty$ or $\beta \rightarrow 1$. The case $\beta \rightarrow -\infty$ applies to all oblate models, and to the outer long axis tubes in prolate models, while the case $\beta \rightarrow 1$ is appropriate for the inner long axis tubes in a prolate model.

APPENDIX E

THE PROJECTED SURFACE DENSITY Σ

In his classic paper, Kuzmin (1956) showed that certain axisymmetric Stäckel models, including the Kuzmin-Kutuzov model studied here, can be written as a weighted sum of perfect spheroids (Z85) with different axis ratios. It follows that the projected surface density of such a model can be written as the same weighted sum of the projected surface densities of the constituent perfect spheroids, each of which is known. In this Appendix we apply this decomposition, and show that the projected surface density of the Kuzmin-Kutuzov model can be given explicitly. As a by-product of the derivation we show that the resulting surface density, when considered as a nonaxisymmetric disk, has a gravitational potential that is of two-dimensional Stäckel form *in* the disk, but not outside it. This is in agreement with the general results on projected Stäckel models obtained by Franx (1988).

Consider a perfect oblate spheroid, with a density distribution given by (see Z85, § III)

$$\rho_{z_c}(\varpi, z) = \frac{M_4}{\pi^2 z_c \varpi_c^2} \frac{1}{[1 + (\varpi^2/\varpi_c^2) + (z^2/z_c^2)]^2}, \quad (\text{E1})$$

where z_c and ϖ_c are constants and M_4 is the total mass. The gravitational potential of this spheroid is of Stäckel form in the spheroidal coordinate system (λ, ϕ, v) , with semifocal distance Δ given by (see § IIa)

$$\Delta^2 = \varpi_c^2 - z_c^2. \quad (\text{E2})$$

Now consider a sequence of these spheroids, with different values of the core radius z_c along the z -axis, and with values of ϖ_c given by

$$\varpi_c^2 - z_c^2 = \Delta^2 = a^2 - c^2, \quad (\text{E3})$$

where a and c are defined in equation (2.3). Since Δ^2 is identical for all these models, the potential of each spheroid is of Stäckel form in the *same* spheroidal coordinate system. Thus, *any weighted sum of density distributions (E1) with z_c and ϖ_c connected by equation (E3) is a mass model with a Stäckel potential.*

Let $\rho(\lambda, \nu)$ be the density distribution of a composite model of the kind we have just described. It is given by

$$\rho(\lambda, \nu) = \int_c^\infty \rho_{z_c}(\lambda, \nu) w(z_c) dz_c, \quad (\text{E4})$$

where $w(z_c)$ is the weight function. Similarly, the G -function that defines the potential via equation (2.5) can be written in terms of the functions G_{z_c} for each of the constituent spheroids as

$$G(\tau) = \int_c^\infty w(z_c) G_{z_c}(\tau) dz_c. \quad (\text{E5})$$

The potential ψ of the model is given by

$$\psi(\lambda, \nu) = \int_c^\infty w(z_c) \psi_{z_c}(\lambda, \nu) dz_c, \quad (\text{E6})$$

where ψ_{z_c} is the potential of an individual spheroid.

Kuzmin (1956) showed that the model defined in § IV can be written explicitly as a weighted sum of the form (E4). In our notation, the appropriate weight function $w(z_c)$ is given by

$$w(z_c) = \frac{Mc^2}{M_4 z_c^2 \sqrt{z_c^2 - c^2}}, \quad (\text{E7})$$

where M is the total mass of the Kuzmin-Kutuzov model. We now use this result to calculate the projected surface density Σ of the elementary model. By definition we have

$$\Sigma = \int_c^\infty w(z_c) \Sigma_{z_c} dz_c, \quad (\text{E8})$$

where Σ_{z_c} is the projected surface density of the spheroid (E1). In what follows, we first calculate Σ_{z_c} , and derive some of its properties, and then we use equation (E8) to find Σ .

View a spheroid (E1) at an angle θ from the z -axis. Since the model is axisymmetric, we may take the viewing direction in the (y, z) -plane without loss of generality. We project along the viewing direction, which we take as the z' -axis, onto a perpendicular plane, which is the (x', y') -plane. The coordinate transformation is

$$x = x', \quad y = y' \cos \theta - z' \sin \theta, \quad z = y' \sin \theta + z' \cos \theta. \quad (\text{E9})$$

The projected surface density $\Sigma_{z_c}(x', y')$ is given by

$$\Sigma_{z_c}(x', y') = \int_{-\infty}^{\infty} \rho_{z_c}(x', y', z') dz'. \quad (\text{E10})$$

Substitution of equations (E1) and (E9) then gives, after a straightforward calculation,

$$\Sigma_{z_c}(x', y') = \frac{M_4}{2\pi\varpi_c(z_c^2 + \Delta^2 \cos^2 \theta)^{1/2}} \frac{1}{[1 + (x'^2/\varpi_c^2) + y'^2/(z_c^2 + \Delta^2 \cos^2 \theta)]^{3/2}}. \quad (\text{E11})$$

This is the density distribution of a perfect elliptic disk with semiaxes $\varpi_c = (z_c^2 + \Delta^2)^{1/2}$ and $(z_c^2 + \Delta^2 \cos^2 \theta)^{1/2}$.

From Z85 we know that the elliptic disk (E11) has a gravitational potential that is of three-dimensional Stäckel form, and hence has an associated ellipsoidal coordinate system (λ', μ', ν') . These coordinates are defined by specification of the positions of their two pairs of foci on the z' -axis, at $z' = \pm \Delta'_1$ and $z' = \pm \Delta'_2$, with

$$\Delta'_1 = \sqrt{z_c^2 + \Delta^2 \cos^2 \theta}, \quad \Delta'_2 = \sqrt{z_c^2 + \Delta^2} = \varpi_c. \quad (\text{E12})$$

In the (x', y') -plane, λ' and μ' are elliptic coordinates, with a pair of foci on the y' -axis, at $y' = \pm \Delta'$, with

$$\Delta' = \Delta \sin \theta, \quad (\text{E13})$$

where—as we have seen— $\Delta^2 = a^2 - c^2 = \varpi_c^2 - z_c^2$ defines the spheroidal coordinates in which the three-dimensional gravitational potential of the perfect spheroid (E1) is of Stäckel form. We write

$$\Delta^2 = \beta' - \alpha', \quad \Delta_1'^2 = \gamma' - \beta', \quad \Delta_2'^2 = \gamma' - \alpha', \quad (\text{E14})$$

with

$$\alpha' = -a^2 \sin^2 \theta, \quad \beta' = -c^2 \sin^2 \theta, \quad \gamma' = z_c^2 - c^2 + a^2 \cos^2 \theta. \quad (\text{E15})$$

Then we have, in the (x', y') -plane,

$$x'^2 = \frac{(\lambda' + \alpha')(\mu' + \alpha')}{\alpha' - \beta'}, \quad y'^2 = \frac{(\lambda' + \beta')(\mu' + \beta')}{\beta' - \alpha'}. \quad (\text{E16})$$

Substitution of these expressions in equation (E11) results in

$$\Sigma_{z_c}(\lambda', \mu') = \frac{M_4(z_c^2 + \Delta^2)(z_c^2 + \Delta^2 \cos^2 \theta)}{2\pi[(\lambda' + \gamma)(\mu' + \gamma')]^{3/2}}. \quad (\text{E17})$$

We remark that, although the (λ', μ', ν') -coordinates depend on both z_c and θ , the elliptic coordinate system (λ', μ') is independent of the value of z_c . Thus, when considered as a perfect elliptic disk, each density (E17) has a potential *in the disk* that is of two-dimensional Stäckel form in *the same* elliptic coordinates. Hence the same is true for any weighted sum of these disks, and in particular for the disk with surface density Σ , given in equation (E8). As a result, *equation (E8) defines not only the projected surface density of the Kuzmin-Kutuzov model, but also a nonaxisymmetric disk with a Stäckel potential in it, although its three-dimensional potential is not separable (since γ' depends on z_c).* Franx (1988) has shown that this result holds for the projection of any three-dimensional Stäckel model.

Now we return to equation (E8) for the projected surface density of the Kuzmin-Kutuzov model. Upon substitution of equations (E7) and (E17) we obtain

$$\Sigma(\lambda', \mu') = \frac{Mc^2}{2\pi} \int_c^\infty \frac{(z_c^2 + \Delta^2)(z_c^2 + \Delta^2 \cos^2 \theta) dz_c}{z_c^2 \sqrt{z_c^2 - c^2} [(\lambda' + a^2 \cos^2 \theta - c^2 + z_c^2)(\mu' + a^2 \cos^2 \theta - c^2 + z_c^2)]^{3/2}}. \quad (\text{E18})$$

It is useful to write $s = z_c^2 - c^2$. This gives

$$\Sigma(\lambda', \mu') = \frac{Mc^2}{4\pi} \int_0^\infty \frac{(s + a^2)(s + c^2 + \Delta^2 \cos^2 \theta) ds}{s^{1/2}(s + c^2)^{3/2}(s + \lambda' + a^2 \cos^2 \theta)^{3/2}(s + \mu' + a^2 \cos^2 \theta)^{3/2}}. \quad (\text{E19})$$

This integral can be evaluated in terms of the incomplete elliptic integrals of the first and second kinds. This can be done, e.g., by use of the tables of Byrd and Friedman (1971). A transparent result is obtained by using Carlson's (1979) symmetric forms R_F and R_D , defined as

$$R_F(x, y, z) = \frac{1}{2} \int_0^\infty \frac{dt}{\sqrt{(t+x)(t+y)(t+z)}}, \quad R_D(x, y, z) = \frac{3}{2} \int_0^\infty \frac{dt}{\sqrt{(t+x)(t+y)(t+z)}}.$$

These functions are available in the standard numerical libraries. The relations with Legendre's incomplete elliptic integrals E and F are

$$F(\varphi, k) = \sin \varphi R_F(q, r, 1), \quad E(\varphi, k) = \sin \varphi R_F(q, r, 1) - \frac{1}{3} k^2 \sin^3 \varphi R_D(q, r, 1), \quad (\text{E21})$$

with $q = \cos^2 \varphi$ and $r = 1 - k^2 \sin^2 \varphi$.

After a straightforward but lengthy calculation we find

$$\begin{aligned} \Sigma(\lambda', \mu') &= \frac{M}{2\pi} \frac{1}{(\lambda' - \mu')^2 (\lambda' + \alpha' + a^2)(\mu' + \alpha' + a^2)(\lambda' + \alpha' + \Delta^2)(\mu' + \alpha' + \Delta^2)} \\ &\times \left\{ P_1(\lambda', \mu') + \frac{3[P_2(\lambda', \mu')R_F(q, r, 1) - P_3(\lambda', \mu')R_D(q, r, 1)]}{(\lambda' + \alpha' + a^2)^{1/2}(\mu' + \alpha' + a^2)^{1/2}} \right\}, \end{aligned} \quad (\text{E22})$$

with

$$\begin{aligned} P_1(\lambda', \mu') &= -c^2(\mu' + \alpha')(\mu' + \beta')(\lambda' + \alpha' + a^2)(\lambda' + \alpha' + \Delta^2) - c^2(\lambda' + \alpha')(\lambda' + \beta')(\mu' + \alpha' + a^2)(\mu' + \alpha' + \Delta^2), \\ P_2(\lambda', \mu') &= -(\lambda' + \alpha' + a^2)(\mu' + \alpha' + a^2) \\ &\quad + [c^2(\mu' + \alpha')(\mu' + \beta')(\lambda' + \alpha' + \Delta^2) + c^2(\lambda' + \alpha')(\lambda' + \beta')(\mu' + \alpha' + \Delta^2) + \Delta^2(\Delta^2 - \Delta'^2)(\lambda' - \mu')^2], \\ P_3(\lambda', \mu') &= c^2(\mu' + \alpha')(\mu' + \beta')(\lambda' + \alpha' + a^2)(\lambda' + \alpha' + \Delta^2)^2 + c^2(\lambda' + \alpha')(\lambda' + \beta')(\mu' + \alpha' + a^2)(\mu' + \alpha' + \Delta^2)^2 \\ &\quad + \Delta^2(\Delta^2 - \Delta'^2)(\lambda' + \alpha' + a^2)(\mu' + \alpha' + a^2)(\lambda' - \mu')^2, \end{aligned} \quad (\text{E23})$$

and

$$q = \frac{c^2}{\lambda' + \alpha' + a^2}, \quad r = \frac{c^2}{\mu' + \alpha' + a^2}. \quad (\text{E24})$$

The expression (E19) is invariant under the formal transformation $\lambda' \rightarrow \mu', \mu' \rightarrow \lambda'$. Upon exchange of λ' and μ' we have $q \rightarrow r$ and $r \rightarrow q$, but R_F and R_D are invariant. The functions P_1, P_2 , and P_3 are symmetric functions of their arguments, so that expression (E22) is invariant upon exchange of λ' and μ' , as it should be.

The expression for the projected surface density simplifies on the y' -axis. In the elliptic coordinates (λ', μ') this axis is given by

$$\begin{aligned} \lambda' &= -\alpha', & \mu' &= y'^2 - \beta', & \text{for } 0 \leq |y'| \leq \Delta', \\ \mu' &= -\alpha', & \lambda' &= y'^2 - \beta', & \text{for } \Delta' \leq |y'|. \end{aligned} \quad (\text{E25})$$

Then we have

$$\Sigma(\lambda', -\alpha') = S(\lambda'), \quad \Sigma(-\alpha', \mu') = S(\mu'), \quad (\text{E26})$$

where

$$S(\tau) = \frac{M}{6\pi a} \frac{1}{(\tau' + \alpha')(\tau' + \alpha' + a^2)^{3/2}(\tau' + \alpha' + \Delta^2)} \{(\Delta^2 - \Delta'^2)(\tau' + \alpha')(\tau' + \alpha' + a^2)[3R_F(q, r, 1) - R_D(q, r, 1)] + c^2(\tau' + \beta')[3(\tau' + \alpha' + a^2)R_F(q, r, 1) - \Delta^2 R_D(q, r, 1) - 3a\sqrt{\mu' + \alpha' + a^2}]\}, \quad (\text{E27})$$

with $\tau' = \lambda', \mu'$, and

$$q = \frac{c^2}{a^2}, \quad r = \frac{c^2}{\tau' + \alpha' + a^2}. \quad (\text{E28})$$

At the foci of the elliptic coordinates we have $\lambda' = \mu' = -\alpha'$, so that $r = q$. In this case the incomplete elliptic integrals reduce to elementary functions, and we find

$$\Sigma(-\alpha', -\alpha') = \frac{M}{6\pi a^2} \left\{ \left[\frac{3}{1-q} - \frac{3q \operatorname{Arth} \sqrt{1-q}}{(1-q)^{3/2}} \right] \cos^2 \theta + \left[\frac{1-3q}{2} + \frac{3q \operatorname{Arth} \sqrt{1-q}}{\sqrt{1-q}} \right] \sin^2 \theta \right\}, \quad (\text{E29})$$

where $q = c^2/a^2$. The central projected surface density is given by

$$\Sigma(-\alpha', -\beta') = \frac{M}{6\pi a} \frac{1}{\sqrt{a^2 - \Delta'^2}} [3R_F(q, r, 1) - R_D(q, r, 1)], \quad (\text{E30})$$

where $q = c^2/a^2$ and $r = c^2/(a^2 - \Delta'^2)^{1/2}$.

If we write equation (E4) in terms of (ϖ, z) instead of (λ, ν) it is evident that the expression for the density of the Kuzmin-Kutuzov model as an integral over perfect spheroids is valid for arbitrary values of c and a . The same is true for the projected surface density Σ . As a result, although the expression (E22) has been derived for $c < a$, i.e., for oblate models, it is valid for the prolate Kuzmin-Kutuzov models as well. In the latter case the x' -axis is the short axis of the projected surface density. The associated elliptic coordinates (λ', μ') have their foci on this axis, in agreement with the fact that the quantities Δ^2 and Δ'^2 are now negative (cf. eqs. [E3] and [E14]).

For $c = a$ the Kuzmin-Kutuzov model reduces to Hénon's (1959) isochrone, and our constituent perfect spheroids are spheres with different core radii. We now have

$$\alpha' = \beta', \quad \mu' = -\alpha', \quad \lambda' + \alpha' = \varpi'^2 = x'^2 + y'^2, \quad (\text{E31})$$

so that

$$q = \frac{a^2}{\varpi'^2 + a^2}, \quad r = 1. \quad (\text{E32})$$

As a result, our expression for Σ reduces to

$$\Sigma(\varpi') = \frac{Ma}{2\pi\varpi'^3} \left(\arctan \frac{\varpi'}{a} - \frac{a\varpi'}{\varpi'^2 + a^2} \right). \quad (\text{E33})$$

This is identical to the result obtained by Hénon (1959) via direct integration. The central projected surface density is equal to $M/3\pi a^2$.

REFERENCES

- Bacon, R. 1985, *Astr. Ap.*, **143**, 84.
 Bertin, G., and Stiavelli, M. 1984, *Astr. Ap.*, **137**, 26.
 Binney, J. J. 1978, *Comments Ap.*, **8**, 27.
 Binney, J. J., and Petrou, M. 1985, *M.N.R.A.S.*, **214**, 449.
 Bishop, J. L. 1986, *Ap. J.*, **305**, 14.
 ———. 1987, *Ap. J.*, **322**, 618.
 Byrd, P. F., and Friedman, M. D. 1971, *Handbook of Elliptic Integrals for Engineers and Scientists* (New York: Springer).
 Camm, G. L. 1941, *M.N.R.A.S.*, **101**, 195.
 Carlson, B. C. 1979, *Num. Math.*, **33**, 1.
 Chandrasekhar, S. 1942, *Principles of Stellar Dynamics* (Chicago: University of Chicago Press).
 Contopoulos, G. 1956, *Zs. Ap.*, **39**, 126.
 Davies, R. D. 1987, in *IAU Symposium 127, Structure and Dynamics of Elliptical Galaxies*, ed. P. T. de Zeeuw (Dordrecht: Reidel), p. 63.
 Dejonghe, H. 1984, *Astr. Ap.*, **133**, 225.
 ———. 1986, *Physics Rept.*, **133**, 218 (D86).
 ———. 1987, *Ap. J.*, **320**, 477.
 ———. 1988, *SIAM J. Applied Math.*, submitted.
 Dejonghe, H., and de Zeeuw, P. T. 1988, *Ap. J.*, **329**, 720.
 de Zeeuw, P. T. 1985a, *M.N.R.A.S.*, **216**, 273 (Z85).
 ———. 1985b, *M.N.R.A.S.*, **216**, 599.
 ———. 1987, in *IAU Symposium 127, Structure and Dynamics of Elliptical Galaxies*, ed. P. T. de Zeeuw (Dordrecht: Reidel), p. 271.
 ———. 1988, *Ap. J.*, to be submitted.
 de Zeeuw, P. T., Hunter, C., and Schwarzschild, M. 1987, *Ap. J.*, **317**, 607.
 de Zeeuw, P. T., and Lynden-Bell, D. 1985, *M.N.R.A.S.*, **215**, 713.
 de Zeeuw, P. T., Peletier, R. F., and Franx, M. 1986, *M.N.R.A.S.*, **221**, 1001.
 Eddington, A. S. 1914, *M.N.R.A.S.*, **75**, 366.
 ———. 1915a, *M.N.R.A.S.*, **76**, 37.
 ———. 1915b, *M.N.R.A.S.*, **76**, 572.
 Erdelyi, A. 1953, *Higher Transcendental Functions*, Vol. 1 (New York: McGraw-Hill).
 Evans, N. W., and Lynden-Bell, D. 1988, *M.N.R.A.S.*, submitted.
 Fillmore, J. A. 1986, *A.J.*, **91**, 1096.
 Franx, M. 1988, *M.N.R.A.S.*, **231**, 285.
 Fricke, W. 1952, *Astr. Nach.*, **280**, 193.
 Fridman, A. M., and Polyachenko, V. L. 1984, *Physics of Gravitating Systems* (New York: Springer).
 Gradshteyn, I. S., and Ryzhik, I. M. 1980, *Table of Integrals, Series, and Products* (New York: Academic).
 Hénon, M. 1959, *Ann. d'Ap.*, **22**, 126.
 ———. 1960, *Ann. d'Ap.*, **23**, 474.
 Hunter, C. 1975a, in *IAU Symposium 69, Dynamics of Stellar Systems*, ed. A. Hayli (Dordrecht: Reidel), p. 195.
 ———. 1975b, *A.J.*, **80**, 783.
 ———. 1977, *A.J.*, **82**, 271.
 ———. 1987, in *Proc. Symposium in Honor of C. C. Lin*, ed. C. Yuan (Singapore: World Scientific), in press.
 Hunter, C., de Zeeuw, P. T., Park, Ch., and Schwarzschild, M. 1988, in preparation.
 Jeans, J. H. 1915, *M.N.R.A.S.*, **76**, 70.

- Kalnajs, A. 1976, *Ap. J.*, **205**, 751.
 Kuzmin, G. G. 1953, *Tartu Astr. Obs. Teated*, **1**.
 ———. 1956, *Astr. Zh.*, **33**, 27.
 ———. 1973, in *Proc. All-Union Conf., Dynamics of Galaxies and Clusters*, ed. T. B. Omarov (Alma Ata: Akademiya Nauk Kazahskoj SSR), p. 71. (English transl. *IAU Symposium 127, Structure and Dynamics of Elliptical Galaxies*, ed. P. T. de Zeeuw [Dordrecht: Reidel], p. 553).
 Kuzmin, G. G., and Kutuzov, S. A. 1962, *Bull. Abastumani Ap. Obs.*, **27**, 82.
 Levison, H. F., and Richstone, D. O. 1985a, *Ap. J.*, **295**, 340.
 ———. 1985b, *Ap. J.*, **295**, 349.
 ———. 1986, *Ap. J.*, **308**, 627.
 ———. 1987, *Ap. J.*, **314**, 476.
 Lynden-Bell, D. 1960, Ph.D. thesis, Cambridge University.
 ———. 1962, *M.N.R.A.S.*, **123**, 447.
 Merritt, D. R. 1985, *A.J.*, **90**, 1027.
 ———. 1987, in *IAU Symposium 127, Structure and Dynamics of Elliptical Galaxies*, ed. P. T. de Zeeuw (Dordrecht: Reidel), p. 315.
 Nagai, R., and Miyamoto, M. 1976, *Pub. Astr. Soc. Japan*, **28**, 1.
 Oort, J. H. 1965, in *Stars and Stellar Systems*, Vol. 5, *Galactic Structure*, ed. A. Blaauw and M. Schmidt (Chicago: University of Chicago Press), p. 455.
 Osipkov, L. P. 1979, *Pis'ma Astr. Zh.*, **5**, 77 (English transl. *Soviet Astr. Letters*, **5**, 42).
 Petrou, M. 1983a, *M.N.R.A.S.*, **202**, 1195.
 ———. 1983b, *M.N.R.A.S.*, **202**, 1209.
 Richstone, D. O. 1980, *Ap. J.*, **238**, 103.
 ———. 1984, *Ap. J.*, **281**, 100.
 Satoh, C. 1980, *Pub. Astr. Soc. Japan*, **32**, 41.
 Schwarzschild, M. 1979, *Ap. J.*, **232**, 236.
 ———. 1982, *Ap. J.*, **263**, 599.
 Stark, A. A. 1977, *Ap. J.*, **213**, 368.
 Statler, T. S. 1987, *Ap. J.*, **321**, 113.
 Stiavelli, M., and Bertin, G. 1985, *M.N.R.A.S.*, **217**, 735.
 Tremaine, S. D. 1987, in *IAU Symposium 127, Structure and Dynamics of Elliptical Galaxies*, ed. P. T. de Zeeuw (Dordrecht: Reidel), p. 367.
 Vietri, M. 1986, *Ap. J.*, **306**, 48.
 White, S. D. M. 1985, *Ap. J. (Letters)*, **294**, L99.

HERWIG DEJONGHE and TIM DE ZEEUW: Institute for Advanced Study, Princeton, NJ 08540